University of Alberta

Observed Sounding Parameters for Strong and Weak Tornadic Storms

by

Tanya Elizabeth Katherine Prozny

A thesis submitted to the Faculty of Graduate Studies and Research
in partial fulfillment of the requirements for the degree of

Master of Science

Department of Earth and Atmospheric Sciences

Edmonton, Alberta
Fall 2008

Your file Votre référence
ISBN: 978-0-494-47393-1
Our file Notre référence
ISBN: 978-0-494-47393-1

Dedication

To my maternal grandmother, Katherine Walyuchow.

Abstract

This thesis investigates whether sounding parameters allow one to distinguish between strong (F2-F5) and weak (F0-F1) tornadoes in southern Ontario. The analysis includes bulk shear for different pressure levels, most-unstable convective available potential energy (MUCAPE), bulk Richardson number (BRN), precipitable water (PW), and storm convergence. The observational dataset consists of 80 tornadic storm events, represented by 60 soundings, that occurred between 1961 and 1996 close to the upper-air sounding site located at Buffalo, New York.

There was no evidence of any skill to distinguish between strong and weak tornadoes based on the observed shear values, MUCAPE, BRN, and storm convergence. The Ontario findings were compared with those reported for central Alberta. They differed in that bulk shear was indicative of greater potential for strong tornadoes in Alberta, which was not evident for Ontario. In both regions, strong tornadoes tend to occur in environments characterized by higher PW values.

Acknowledgements

I would like to acknowledge Dr. G. W. Reuter for his guidance and direction in helping me prepare this thesis, and also thank him for his endless patience and understanding throughout this project.

I would also like to thank Dr. David Sills from Environment Canada for providing the Ontario tornado dataset used in this thesis.

Financial support for this research was provided by the Natural Sciences and Engineering Research Council and the Canadian Foundation for Climate and Atmospheric Sciences.

Table of Contents

List of Tables

List of Figures

CHAPTER ONE

Introduction

1.1 Introduction to research topic

Tornadoes are rapidly rotating winds that blow around a small area of intense low pressure. The circulation of a tornado is visible on the ground either as a funnel-shaped cloud or a swirling cloud of dust and debris. Of all weather systems, tornadoes are the most violent. The diameter of a tornado is typically between 100 and 600 meters, and it usually rotates cyclonically with wind speeds between 60 km h^{-1} and 200 km h^{-1}. However, wind speeds as high as 500 km h^{-1} have been recorded. The damage of tornadoes is caused primarily by their violent winds and airborne objects. Tornado damage includes blown down trees, utility poles, buildings and other structures. Many deaths associated with tornadoes are caused by flying debris. Broken glass, splintered lumber and even vehicles can become deadly projectiles when subjected to such extreme winds. The updraft near the centre of the storm's funnel may reach 160 km hr^{-1} and be strong enough to lift railroad cars off their tracks or a house off its foundation. More often than not the most destructive of all tornadoes are those with multiple vortexes that orbit about each other or about a common vortex centre.

Most tornadoes are small, short-lived and often strike sparsely populated areas. Occasionally, however, tornado outbreaks can cause incredible devastation, death and injury and radically impact the lives of people. Typically the path length of a weak tornado is less than 1.6 km long and 100 m wide and it typically exists for only a few minutes with wind speeds that are less than 180 km

h^{-1}. Over three-quarters of tornadoes that occur are considered weak, but they account for only 5% of tornado fatalities. On the other extreme, violent tornadoes can have damage paths that are more than 160 km long and 1 km wide, and the lifetime of these storms may be anywhere from ten minutes to two hours. Such intense storms have wind speeds of up to 500 km hr^{-1} and cause 95% of deaths associated with tornadoes (Moran 2006). A six-point intensity scale for rating tornado strength based on damage to structures was devised by T. T. Fujita in 1981 (Table 1). Termed the F-scale, it is based on rotational wind speeds estimated from property damage. This scale categorizes tornadoes as weak (F0, F1), strong (F2, F3), or violent (F4, F5).

Table 1: The Fujita Tornado Intensity Scale with corresponding wind speed (estimated) and typical damage for each storm category. Adapted from Moran, 2006 and the Storm Prediction Center website at http://www.spc.noaa.gov/faq/tornado/f-scale.html.

F-scale	Category	Wind Speed (km hr^{-1})	Typical Damage
0	Weak	65-118	Snaps twigs and small branches, pushes over shallow-rooted trees, breaks some windows, damages sign boards.
1		119-181	Downs trees, peels surface off roofs, shifts mobile homes off foundations or overturns them, blows moving autos off roads.
2	Strong	182-253	Rips roofs off frame houses, demolishes mobile homes, uproots or snaps large trees, generates light-object missiles.
3		254-332	Partially destroys well-constructed buildings, lifts and throws motor vehicles, uproots most trees in forest.
4	Violent	333-419	Levels sturdy buildings and other structures, tosses automobiles about like toys, generates large missiles.
5		420-513	Lifts and sweeps away strong frame houses, throws automobile-sized missiles 100+ m, debarks trees.

In Canada, most tornadic storms occur in southern Ontario and central Alberta. The majority of them are weak tornado cases. Strong tornadoes are rare, while violent tornadoes are extremely rare. Since the prospect of fatalities and major property damage is much greater for strong and violent tornadoes, it would be of interest to a forecaster to be able to assess the probability that a tornado outbreak would be severe. Traditionally, research has been undertaken to assess the likelihood of the occurrence of tornado formation. The search was to identify relevant atmospheric parameters that would allow a forecaster to distinguish between tornadic and non-tornadic thunderstorms. Dupilka and Reuter (2006a, b), however, have recently shifted the focus to identify the likely intensity of a predicted tornado. Sounding parameters were indentified with appropriate threshold values that provide reliable insight into the likely occurrence of strong tornadoes versus weak tornadoes in central Alberta.

This thesis research is an extension of Dupilka and Reuter's research. Whereas that study dealt with weak and strong tornadoes observed in central Alberta, this investigation is focused on tornadic storm events that took place in southern Ontario. The observational dataset spans from 1961 to 1996. The focus of this study is on whether it is possible to determine the likelihood of occurrence of strong versus weak tornadoes based on different environmental conditions. Ultimately, the goal of this research is to develop tools and provide knowledge for operational weather forecasters in southern Ontario to be alert as to the conditions under which tornadoes become life-threatening, as this region has the highest tornado occurrence as well as the highest population density in

Canada. This will allow for the timely issue of tornado warnings to the public and provide the opportunity for emergency response to take appropriate action and conceivably save human lives.

1.2 Theory of tornado formation

Analysis of observed data sampled in the vicinity of tornadic storms has identified several necessary conditions required for the formation of thunderstorms that can spawn tornadoes. These necessary conditions for tornadic storms are very similar for those required for the formation of severe supercell thunderstorms or intense multicell storms. The necessary conditions are (Verkaik and Verkaik, 1998):

1) a large amount of convective available potential energy (CAPE),
2) a large amount of atmospheric moisture,
3) strong vertical shear of the horizontal wind for storm organization,
4) a triggering mechanism.

CAPE is the energy (per unit mass of air) that is potentially available for storm development, i.e. the amount of latent energy that can be converted into heat and subsequently into kinetic energy. CAPE is equal to half the square of the maximum updraft speed sustainable by convection. The total amount of atmospheric moisture can be quantified by the precipitable water (PW), which is defined as the mass of water vapour contained in a vertical column of air with unit cross-sectional area. In order to tap into the stored latent energy within the water vapor, sufficient lifting is needed to allow for adiabatic cooling to convert

the vapor into liquid cloud water at the condensation level and above. This is accomplished as soon as air parcels achieve sufficient lift to break the capping inversion via some sort of triggering mechanism; such as frontal lift, outflow boundaries of existing thunderstorms, convergence lines, surface heating, upper or mid-level divergence, and others (Etkin 2001). Once a thunderstorm has formed, considerable vertical wind shear is needed for the organization of severe storms to allow for a separation of the inflow updraft region and the outflow downdraft region. Without wind shear, the downdraft forms vertically above the updraft and terminates the ascending air and condensation. The vertical wind shear vector can consist of both speed shear and directional shear. Speed shear denotes the difference in wind speed between two levels, whereas directional shear denotes the change of direction of the wind vectors from the bottom and top of the layer. A wind vector that changes direction in a clock-wise motion is said to veer. Generally, larger shears and veering winds with height are necessary in order to intensify and prolong the persistent rotating updrafts that characterize severe tornadic thunderstorms (Darkow and Fowler 1971). Typically, environmental conditions favoring tornado formation feature a balance between the strength of wind veering and the amount of atmospheric stability (Schaefer and Livingston 1988).

While scientists are aware of these necessary conditions for severe storm formation and tornadogenesis, the sufficient conditions for tornado formation are not known. Furthermore, there remains considerable uncertainty about the physical mechanisms that cause tornadogenesis. In their study, Verification of

the Origins of Rotation in Tornadoes Experiment (VORTEX), Rasmussen et al (1994) review some theories regarding tornadoes and tornadogenesis. Usually, updrafts in supercell thunderstorms begin to rotate at mid-levels when horizontal vorticity, generated by strong low-level environmental wind shear, is tilted into the vertical (e.g. Klemp 1987). The horizontal vorticity develops a large stream-wise component in the same direction as the storm-relative wind when, in the lowest few kilometers, the storm-relative winds veer significantly in a clock-wise direction. The initial mid-level mesocyclone is formed when the updraft tilts this stream-wise vorticity into the vertical (Davies-Jones 1984). If the low-level, storm-relative winds are strong enough, updraft rotation is prolonged because the storm's cold outflow would be prevented from surging ahead of the storm, which would effectively cut the updraft off from its low-level source of warm, moist air.

This does not explain, however, how rotation develops at near-ground levels, i.e., near 2 km AGL. From numerical simulations, Rotunno and Klemp (1985), Klemp (1987), Davies-Jones and Brooks (1993) and Markowski et al. (2002) found that the development of low-level mesocyclone rotation is a separate process which may depend on the initial formation of a rain-cooled downdraft. Rotation is first suspected to develop in evaporatively cooled subsiding air just behind the gust front on the left, rear side of a mesocyclone (when viewed from the rear). Initially, spiraling rain curtains and a corresponding downdraft form within the mid-level mesocyclone. In the lowest kilometer, rapidly subsiding rain-cooled air can acquire sizeable stream-wise horizontal vorticity

generated by differences in buoyancy between cool air within the downdraft and relatively warmer on its fringe. However, the extent to which low-level mesocyclones contribute to the formation of tornadoes is uncertain. Rasmussen et al. (1994) speculated that low-level and mid-level mesocyclones merge allowing for intensification and deepening of circulation.

Another possible mechanism is that tornadogenesis originates from substantial horizontal vorticity generated by extreme horizontal wind shear between the rapidly rising air on the edge of an updraft core and the relatively small vertical motions just outside of it. This shear instability may cause "vorticity rolls" to develop along the boundary which will be further enhanced and brought down to the surface by the development of a downdraft. As subsiding air reaches the surface, it is spread out allowing some air to move forward and become entrained into the main updraft's right rear side where its vorticity is increased by vertical stretching within the updraft. Thus, cyclonically spinning air is transported downward along the ground and into the side of the updraft, which is significant because tornadoes typically form in this area near the interface between the updraft and downdraft. This mechanism may be a plausible explanation as to how many of the stronger tornadoes develop from mesocyclones, but it may not account for the generally weaker, and greater in number, tornadoes that do not form from mesocyclones. Wakimoto and Wilson (1989) hypothesize that non-mesocyclone tornadoes may be formed by horizontal shear instabilities along convergence lines which generate vertical vorticity and cause individual vortexes to form. If these vortexes, as they

propagate along the convergence line, happen to collocate with the updraft of a rapidly developing storm, they are stretched upwards allowing them to strengthen to possible tornadic intensity.

However, as stated earlier, there still does not exist a definitive model of tornadogenesis despite much progress in the past 25 years. It is uncertain which factors are necessary for tornado formation and which of these factors affect tornado intensity. It is also uncertain as to whether or not non-tornadic severe thunderstorms form in environments noticeably different from tornadic storms, and whether the intensity of tornadic storms is related to certain environmental characteristics. The aim of this research is to determine whether there are any differences in the environments which support strong versus weak tornadoes.

1.3 Ontario tornado climatology

Figure 1.1 shows the annual average number of tornadoes across Canada per 10 000 km^2 (Newark 1984). The figure depicts that southern Ontario is the region of greatest tornadic activity in Canada, experiencing 2.5 to 4.9 tornadoes per year per 10 000 km^2. Etkin (2001) comments that the region of frequent tornado occurrence in southern Ontario is the northern extension of "tornado alley" which stretches from Texas to the Midwest of the United States. Figure 1.2 shows the location of tornadoes for Ontario between 1918 and 2003. The dot colors indicate the estimated tornado intensity on the Fujita F-scale. The observations show that the number of tornado events decreases from south to north, i.e. northern Ontario sees less tornadoes than southern Ontario. Most

tornadoes occurring in Ontario are weak, rated at F0 or F1 on the Fujita scale, and the majority of strong tornadoes in Ontario (F2 or greater) occur within a narrow expanse of land which is commonly referred to as Canada's tornado alley (Etkin 2001).

The finding that an increase in latitude is associated with a decrease in observed tornado events is consistent with observations of other convective storm phenomena. Figure 1.3 shows the geographical frequency distribution of average annual lightning flash density (Figure 1.3a) and hailfall events (Figure 1.3b). In comparing Figure 1.2 with Figure 1.3, it is evident that the area of highest tornado frequency in Ontario agrees well with the areas of highest lightning activity and hail fall events.

Not all tornadoes in Ontario are spawned from supercell storms (Etkin 2001). Sills (1998) suggests that summertime convective storms in Ontario are often caused by lake-breeze boundary convection. The location and timing of sea breeze convection tends to coincide with tornado observations. While it is possible to make a general description of storm environments to explain large-scale climatological patterns, severe storm and tornado formation are largely dependent on the local environment, and this study is an attempt to examine the local environment by investigating the use of observed environmental sounding parameters to assess the potential for severe storm development.

1.4 Forecasting of tornadoes

One of the primary responsibilities of Environment Canada is to issue timely warnings for extreme weather events such as severe thunderstorms with the likelihood of tornadoes and/or large hail. Most weather forecasters focus on a time window of three to twelve hours for issuing the likelihood of extreme weather. Operational forecasters utilize three techniques to assist them in assessing the risk for violent thunderstorms:

1) guidance from numerical weather prediction models,
2) conceptual models of severe storms,
3) ingredients-based approaches.

Numerical models useful for this purpose simulate synoptic and mesoscale processes, while conceptual models rely on correlating synoptic and mesoscale patterns with similar weather events. An ingredients-based approach, however, aims to assist the forecaster in deciding the potential for severe weather by investigating various atmospheric parameters, which are physically related to storm development, in a probabilistic manner. The research in this thesis concentrates on this last approach.

Numerical weather prediction models have been steadily improving in recent years due to increasing computational resources. The horizontal resolution currently achievable amounts to a grid spacing of about 10 km. However, modeling thunderstorm updrafts/downdrafts, and subsequent tornadoes, would require computations to be done on a much smaller scale (on the order of 100 m), which cannot be attained using current computational

resources. In order to evaluate the physical processes involved in tornadogenesis, cumulus-scale models were developed capable of simulating tornadic storms (Schlesinger 1975, Klemp and Wilhelmson 1978) and tornadoes (Rotunno 1979). These non-hydrostatic models have continued to increase in complexity such that numerical modeling of tornado-like vortexes is now possible (Orf and Wilhelmson 2004). However, these tornado simulations require several days of computing time on current-generation supercomputers and are thus not practical for an operational forecasting environment. Also, current operational data collection does not yield sufficient data to adequately provide the high-resolution initial conditions necessary for these storm models.

Conceptual models involve incorporating many physical parameters into a type of blueprint to generally describe meteorological events such as thunderstorm outbreaks. These physical parameters are gathered via a large number of observations related to similar weather events which are then combined in order to describe the situation most probable to occur. Thus, it is not surprising that conceptual models often fail to forecast violent storm events. One conceptual model that has been useful for the last 25 years is a conceptual model of a supercell thunderstorm developed by Lemon and Doswell (1979). Features of this model include the description of a mesocyclone characterized by a hook shaped radar reflectivity region which surrounds a cyclonically rotating updraft that changes into a divided mesocyclone with a downdraft on the rear flank and updraft on the forward flank; the more significant tornadoes develop on the boundary separating positive and negative velocity. It also includes a

description of a surface gust front structure resembling that of an extratropical cyclone. This model is widely used by operational forecasters and can be useful for making quick decisions regarding the potential for severe convective development. However, one must be careful not to use such models rigidly and therefore reject outcomes which may not necessarily fit the model precisely. It is important, then, for a forecaster to possess thorough knowledge of the physical processes involved as well as the limitations of existing theories in order to better gauge the potential for severe thunderstorms and possible tornadoes.

Another, more sophisticated method of determining the potential for violent storm formation is through an ingredients-based approach which examines several parameters physically related to storm development. Storm parameters computed from observed soundings (or model predicted soundings) have been examined by Colquhoun and Shepherd (1989), Brooks et al. (1994), Rasmussen and Blanchard (1998), Thompson et al. (2003), and others. The sounding parameters investigated include vertical shear in the horizontal wind, thermal buoyancy, atmospheric humidity, storm-relative helicity, and others. This study uses an ingredients-based method to examine various environmental parameters associated with tornadic storm events in order to discriminate between the intensity of tornadoes.

The use of proximity soundings to assess environmental parameters related to mesoscale supercells and tornadoes has been widely used. Early work by Darkow and Fowler (1971) examined the role of vertical wind shear to distinguish severe storms. Colquhoun and Shepherd (1989) studied the

relationship between wind shear and tornado intensity. Rasmussen and Wilhelmson (1983) as well as Monteverdi et al. (2003) investigated parameters involving shear and buoyancy. Rasmussen and Blanchard (1998) created a proximity sounding climatology of supercell and tornado parameters including wind shear, buoyancy, and combinations thereof, in order to investigate the use of environmental sounding parameters to distinguish between non-tornadic storms, weak tornadoes and strong tornadoes. The same distinction was made by Thompson et al. (2003) through using numerically generated soundings to calculate various parameters, (including shear, buoyancy and helicity), as well as Davies (2004) who investigated the use of sounding calculated buoyancy parameters. Dupilka and Reuter (2006a, b) computed sounding parameters for proximity soundings for Alberta tornadoes. Their study investigated wind shear for different layers, thermal buoyancy, helicity, precipitable water (PW), and storm convergence to distinguish between non-tornadic severe thunderstorms, thunderstorms with weak tornadoes (F0-F1), and thunderstorms with significant tornadoes (F2-F5).

Due to the potential for tornadoes to cause extreme damage, serious injuries and death, it is important to improve the reliability of forecasted tornado warnings. A useful tool for operational forecasters in Canadian weather offices would be to have criteria that might help to distinguish between sounding environments that favor strong tornadic storms versus weak tornadic storms. It should be cautioned, however, that this research does not attempt to promote "magic numbers" as a method of forecasting, but instead seeks to gain new

physical insight into the large scale influences on supercell storms and provide the forecaster with additional tools to assess the potential for tornadic storm development (Rasmussen and Blanchard 1998).

1.5 Thesis objectives

The focus of this research is on determining whether observed environmental sounding parameters can be used to assess the likelihood that tornadic storms in southern Ontario will be weak (F0, F1) or strong (F2, F3, F4). These results for southern Ontario will then be compared with results from Alberta compiled by Dupilka and Reuter (2006a, b). The two specific objectives investigated in this thesis are:

1) Are there differences between the sounding environments of strong and weak tornadic storms in southern Ontario? In particular, are there differences between storm parameters such as bulk and directional wind shear, convective available potential energy, bulk Richardson number, precipitable water and storm convergence?

2) Are there differences between the soundings supporting strong versus weak tornadic storms in Ontario and Alberta? In particular, are there differences between the magnitudes and ranges of sounding parameters such as bulk wind shear, CAPE, precipitable water and storm convergence?

This thesis will analyze observed sounding data from Buffalo, New York and then compare it to analysis done on sounding data from Stony Plain, Alberta by Dupilka and Reuter (2006a, b).

Chapter two begins with essential background information on the radiosonde network and the use of radiosonde data. Additional information on this topic is contained in appendixes A and B. The chapter continues with a discussion of the database used to obtain the dataset and the ways in which data was selected for the study. This is followed by a detailed description of each sounding parameter examined in the study and how their values were determined.

Chapter three contains a discussion of the significance of these parameters including past research. The results of the sounding analysis for tornadic storms in southern Ontario are presented for each sounding parameter. The use of the parameters introduced in chapter two to distinguish between environments that support strong versus weak tornadoes in Ontario is investigated.

In chapter four, the results for tornadic storms in Ontario are compared with the sounding analysis completed for Alberta by Dupilka and Reuter (2006a, b). The focus is on determining if there are any differences in storm environments which support strong versus weak tornadic storms in Ontario and Alberta.

The final chapter contains a summary of the results, a brief discussion on the importance of the research and offers some suggestions for further research.

Following the final chapter is some additional material contained in appendixes. As stated earlier, appendix A and B contain additional information on the radiosonde network and the use of data obtained by radiosondes. Appendix C is a detailed list of all tornado events in the study including the date and time of occurrence, location, and distance from the upper-air site, BUF. Appendix D contains a chart on hail size conversion and Appendix E contains some comments on specific data points that were eliminated from the study.

CHAPTER TWO

Database and Method of Analysis

This chapter contains information about the radiosonde network and the use of radiosonde data for analysis. Thereafter is a discussion of the database used to obtain the dataset for the study, and the methods in which the data were selected. This is followed by a description of the sounding parameters used in the study, including bulk and directional wind shear, convective available potential energy (CAPE), the bulk Richardson number (BRN), precipitable water (PW), and storm convergence.

2.1 Radiosonde network

Observations suggest that the type and intensity of thunderstorms depend on the characteristics of the vertical distribution of heat, moisture and momentum. The most crucial sounding parameters include wind shear, CAPE and PW (Dupilka and Reuter 2006a). To collect this data, meteorologists rely on a balloon-borne instrument platform called a radiosonde (see appendix A).

Measurements collected by the radiosonde sensors are sent by radio signals back to the launching site, where they are received and processed. The observed sounding data are submitted to the world-wide communications network that shares meteorological information around the globe. As stipulated by the World Meteorological Organization (WMO), balloon soundings are released from hundreds of upper-air stations twice daily just prior to 0000 UTC

(Coordinated Universal Time) and 1200 UTC. Thus, worldwide, agencies launch their instruments at approximately the same time, and over 1500 such observations are taken daily (National Weather Service, 2007).

A map of upper-air stations in eastern Canada and the Great Lakes region of the United States is shown in Figure 2.1. The WMO recommends a minimum spacing between upper-air stations of approximately 250 km over large land areas and approximately 1000 km over sparsely populated and oceanic regions. In Canada, however, this spatial requirement is not often followed; some neighboring upper-air sites are separated by 600 km or more (e.g. The Pas, Manitoba (CYQD) to Pickle Lake, Ontario (CYPL)) (Dupilka 2006).

All radiosonde observations of temperature, pressure, humidity and horizontal wind are recorded at standard pressure levels, which are: 1000, 925, 850, 700, 500, 400, 300, 200, 150, 100, 70, 50, 30, 20 and 10 mb. In addition, sounding measurements are documented for the following mandatory levels: the surface; the height at which the balloon burst; one level between 100 and 110 mb; the tropopause; the bases and tops of temperature inversions and isothermal layers greater than 200 mb in thickness and at pressures greater than 300 mb; the bases and tops of all inversion layers with temperature changes of 2.5 °C or 20% relative humidity at pressures greater than 300 mb; levels describing layers with missing or questionable data (Dupilka 2006).

Data gathered by a radiosonde describes the vertical structure, or profile, of the atmosphere. In order to study these data, the observed temperature, dewpoint and relative humidity at selected pressure levels are plotted on

thermodynamic diagrams which are referred to as soundings. For further discussion on thermodynamic diagrams including an example of sounding data and the corresponding diagram, refer to Appendix B.

2.2 Database and data selection

The storm climatology dataset for this study consists of 60 soundings representing 80 tornado events occurring in southern Ontario between 1961 and 1996. Figure 2.2 shows the geographic location of concern in this study. The circle marks a 200 km radius from Buffalo, New York (BUF) since this is the nearest upper-air station. Within this 200 km threshold, 43 tornado events occurred and their representative soundings were used in the dataset. Tornado events which occurred between 200 km and 300 km from BUF were chosen for the dataset if they met the *boundary layer wind vector* criteria defined by Rasmussen and Blanchard (1998). (See figure 1 in Rasmussen and Blanchard 1998). An additional 17 events and corresponding soundings were included based on this criteria (see Appendix C). Any events that occurred at unknown distances from BUF were not included in the dataset.

The data for this study have been provided by the Meteorological Service of Canada (MSC). The data have been gathered by a variety of sources including volunteer severe weather observers, newspaper archives, damage surveys, videos, photographs and eyewitness accounts (Auld et al. 2004). According to the MSC, it is difficult to distinguish between damage caused by non-tornadic and tornadic winds. Therefore, some events classified as tornadoes in Newark's

(1983, 1984) database, particularly for weaker events (i.e. F0 or F1 tornadoes), may in fact be non-tornadic severe storm damaging winds such as downbursts or microbursts (Auld et al. 2004).

The proximity soundings used throughout this research were chosen for those days on which tornado events occurred. Following Dupilka and Reuter (2006a, b), a tornado event was taken to be a single tornado rather than separate sightings of the same tornado. Thus, when separate locations in close proximity report the occurrence of a tornado, it is assumed to be separate sightings of the same tornado and a single event. For such occurrences, the location in which the greatest damage occurred was used for the F-scale damage rating. Also, when more than one tornado event occurred on the same day, the representative sounding was used only once in the dataset corresponding to the highest F-scale rated tornado that occurred within the distance criteria. All tornado events that occurred in southern Ontario prior to 1961 were eliminated as no soundings were available in Buffalo prior to 1961.

The MSC dataset records the time of day for tornado occurrences for most events. As in Dupilka and Reuter (2006a, b), the 0000 UTC sounding corresponding to the day of the event was chosen for the study, provided the storm occurred within $\pm$ 6h of 2000 local daylight time. Since the average time for tornado occurrence is 1743 local time for all Ontario tornadoes in the MSC dataset from 1961-1996, events that occurred at unknown times were included in the study.

The above mentioned spatial and temporal constraints were chosen in order to maintain a reasonable amount of tornado events for the study. Stronger constraints might provide better quality proximity soundings, though the dataset would be smaller.

To further ensure the soundings were representative of the storm environment, additional constraints were applied. Each sounding included in the study was inspected using an extensive software package called RAOB (radio-observation) provided by Environmental Research Services (Shewchuk 2002). Following Dupilka and Reuter (2006a, b), soundings were rejected if the most-unstable CAPE (Doswell and Rasmussen 1994) was less than 50 J kg^{-1}. This requirement eliminated soundings that may be indicative of non-tornadic wind events such as microbursts.

All of the above restrictions resulted in a dataset which includes 60 soundings representing a total of 80 tornado cases (see Appendix C) while eliminating 131 storm events. As noted by Dupilka and Reuter, the choices represent the difficulties associated in obtaining a sufficiently large dataset for rare events while still maintaining a reasonable proximity from the balloon launching site. Figure 2.3 shows the frequency of tornado occurrence versus Fujita scale (F-scale) for the events included in the dataset. As indicated by the figure, weak tornadoes dominate while there are much fewer strong cases. Out of the 60 total storm soundings, there were 32 for F0 tornadoes, 18 for F1 tornadoes, 5 for F2 tornadoes, 3 for F3 tornadoes and 2 for F4 tornadoes. There has not been an F5 tornado reported in Ontario. Also shown in the figure is a solid line indicating the

frequency of F-scale tornadoes in Canada from 1958-1998 (Brooks and Doswell 2001). Approximately 32% of Canadian tornadoes occur in Ontario (Etkin et al 2001). It is evident from the figure that the frequency distribution for Ontario is similar to that of Canada as a whole. For this study, the tornadic events were categorized into two separate classes as per Thompson et al (2003) and Dupilka and Reuter (2006a, b), with strong tornadic events (ST) consisting of F4, F3 and F2 tornadoes and weak tornadic events (WT) consisting of F1 and F0 tornadoes. This resulted in 17% ST cases and 83% WT cases; for the entire Canadian dataset the ratios are similar: 18% ST and 82% WT.

2.3 Computation of sounding parameters

Most of the analysis of soundings was conducted using the RAOB sounding software. This package, developed by Environmental Research Services, is widely used by operational weather offices and storm researchers alike. This software was used to analyze sounding parameters for the Buffalo (BUF) soundings used in this study. The sounding data were obtained from a CD-ROM entitled Rawinsonde Data of North America 1946-1996. The sounding data are also available online at http://raob.fsl.noaa.gov. The parameters included in the study are bulk and directional wind shear, CAPE and bulk Richardson number, precipitable water and storm convergence. The following sections describe how each of these parameters are defined and computed.

2.3.1 Bulk wind shear

The sounding data archives wind measurements at fixed pressure levels. Therefore, bulk wind shear (SHR) was computed using the equation,

$$SHR = \frac{\sqrt{(u_2 - u_1)^2 + (v_2 - v_1)^2}}{|z_2 - z_1|}, \tag{2.1}$$

where (u) and (v) represent the zonal and meridional wind vector components at pressure levels 1 and 2, and (z) is the height (Dupilka 2006). Following Dupilka and Reuter (2006a, b), the bulk shear was calculated for the layers from 900 mb to 800 mb, (signified by SHR8), 900 mb to 700 mb (SHR7), 900 mb to 600 mb (SHR6) and 900 mb to 500 mb (SHR5). The 900 mb wind from the sounding rather than the surface-based wind observation was used to calculate bulk shear so as to avoid surface complexities due to variability in terrain (Dupilka and Reuter 2006a). It should be mentioned that some previous studies have calculated wind shear for specific altitudes instead of pressure levels (e.g. Brooks et al. 1994, Thompson et al 2003). However, since pressure levels are commonly used by forecasters, it is more convenient to select standard pressure levels rather than pre-selected fixed altitudes.

2.3.2 Directional wind shear

To account for both speed and directional shear, i.e. the amount of veering of the wind vector, a parameter first introduced by Colquhoun and Shepherd (1989) called INIS was used (Dupilka and Reuter 2006a). INIS is calculated by

determining the length of a hodograph between two pressure levels (see Figure 2 in Colquhoun and Shepherd 1989). It is given by:

$$INIS \equiv \frac{\left|\sum\left[IN(L)\cdot\Delta p\right]\right| + \left|\sum\left[IS(L)\cdot\Delta p\right]\right|}{\sum\Delta p\sum\left|\Delta z\right|}, \tag{2.2}$$

where $IN(L) = \left|\mathbf{V}_p\right|\sin\theta$ and $IS(L) = \left|\mathbf{V}_p\right|\cos\theta - \left|\mathbf{V}_{p+\Delta p}\right|$. $IN(L)$ and $IS(L)$ are the components of the wind shear vector in a given layer L, normal to and in the direction of the base layer wind, respectively. The angle θ is the angle between the wind vectors $\mathbf{V}_p$ and $\mathbf{V}_{p+\Delta p}$ at pressure levels p and $p+\Delta p$. In this equation, $IN(L)$ relates to directional shear and $IS(L)$ relates to speed shear (Dupilka and Reuter 2006a). INIS was calculated between p and $p+\Delta p$, where Δp corresponds to 50 mb increments and Δz was the height difference between two pressure levels. Similar to bulk shear and following Dupilka and Reuter (2006a,b), INIS values were calculated for the layers 900 mb to 800 mb, 900 mb to 700 mb, 900 to 600 mb and 900 to 500 mb.

2.3.3 Convective available potential energy (CAPE) and bulk Richardson number (BRN)

According to pa`rcel theory (e.g. Rogers and Yau 1996), convective available potential energy (CAPE) is defined as the maximum buoyant energy available to an ascending parcel of air to accelerate it vertically, i.e., it represents the potential energy that may be converted into kinetic energy of rising air parcels. In theory, CAPE is expected to occur whenever unstable layers exist. Thus, the higher the CAPE, the more unstable the atmosphere and the more

energy available for storm development. Parcel theory states that the amount of CAPE can be used to estimate the maximum possible updraft speed of a convective element under the assumption that:

- the parcel is uniform and maintains its identity throughout the thermodynamic process,
- the parcel does not mix with the environment,
- the atmosphere does not compensate for the parcel's motion,
- the parcel and environment are in dynamic equilibrium, meaning the parcel instantaneously adjusts its pressure to equal that of the environment.

The weight of the condensed water carried along with the air parcel is also neglected (e.g. Rogers and Yau 1996). Under these assumptions, the thermal buoyancy of an air parcel, B, is given by

$$B \equiv \frac{T - T'}{T'}, \tag{2.3}$$

where T is parcel's temperature and T' is the temperature of the environment. The vertical velocity $w(z)$ of the air parcel at a height z above the level of free convection z_0 can then be calculated using the formula

$$w^2(z) = w_0^2 + 2g\int_{z_0}^{z} \frac{T - T'}{T'} dz, \tag{2.4}$$

where, by definition, the CAPE between the levels z_0 and z is

$$CAPE \equiv g\int_{z_0}^{z} \frac{T - T'}{T'} dz. \tag{2.5}$$

CAPE represents the work an air parcel does on its environment and is equivalent to the area on a thermodynamic sounding bounded between the environmental temperature and the temperature of an undiluted parcel rising via a moist adiabat from height z_0 to z.

Figure 2.4 shows a typical sounding in the form of a Skew $T - \log p$ diagram for Buffalo, New York (BUF) on April 21, 1996 (data listed in appendix B, table B.1). The solid curve on the sounding indicates the temperature in °C and the dotted red curve indicates the dewpoint temperature in °C. The ascent path of the parcel is shown as a cyan curve on the far right, and the red shaded area represents the CAPE. The value of CAPE depends on the level of free convection (LFC) which is determined by knowing the temperature and dewpoint in the boundary layer. Three different methods are used by the research community to determine the best values for initial temperature and dewpoint to be used in the integration. They are:

1) the surface-based method,
2) the parcel layer method,
3) the most-unstable method.

The surface-based method uses the initial parcel temperature and dewpoint at the surface. The parcel-layer method uses average values of temperature and mixing ratio in a defined boundary layer to estimate the parcel temperature and dewpoint. Usually the layer thickness is chosen to be 100 mb. The most-unstable (MUCAPE) method utilizes the most unstable air parcel in the lowest 300 mb of the sounding (Doswell and Rasmussen 1994). This method generally

provides the maximum amount of CAPE as the LFC is usually calculated to be lower than it is using the other methods. It is useful because sometimes the surface values of temperature and dewpoint are inappropriate, as during nocturnal inversions (Dupilka 2006). In this study, CAPE is calculated using the most-unstable method.

Yet another factor to consider in the determination of CAPE is whether to include the buoyancy effects of different water vapor mixing ratios between the (moister) parcel air and the ambient (drier) air of the sounding. To include the humidity buoyancy effect, one can make an adjustment to the virtual temperature, T_v, instead of temperature, T, in equation (2.5). The virtual temperature is defined by, $T_v \equiv T(1+\varepsilon q)$, where $\varepsilon = 0.608$ is the given the specific humidity, q, (approximately equal to the mixing ratio), expressed in $\frac{g}{g}$ (Rogers and Yau 1996). In the equation of state, $p = \rho R T_v$, p is pressure, ρ is the air density, R is the gas constant for dry air, and the proper temperature to use is the virtual temperature, T_v, such that the gas constant is indeed constant and equal to $287\ \frac{m^2}{s^2 K}$. The virtual temperature correction is always positive and is considered equivalent to warming an air parcel as water vapor is added and it is less dense (Dupilka 2006). Thus the virtual temperature correction can be applied to the computation of densities when calculating CAPE, which relates to the difference in air density between a rising air parcel and its environment (Dupilka 2006). Using this correction, equation 2.5 becomes

$$CAPE \equiv g \int_{z_0}^{z} \frac{T_v - T_v'}{T_v'} dz = R \int_{p}^{p_0} (T_v - T_v') d\ln p . \qquad (2.6)$$

Doswell and Rasmussen (1994) discuss the effect of neglecting the virtual temperature correction.

The bulk Richardson number (BRN) is a parameter which takes into account both convective stability and wind shear. It is defined by Weisman and Klemp (1982) as

$$BRN = \frac{CAPE}{\frac{1}{2}\left(\overline{U}^2 + \overline{V}^2\right)}, \qquad (2.7)$$

where $\overline{U}$ and $\overline{V}$ are the components of the difference between pressure-weighted mean wind from the surface to 6 km above ground level (AGL) and the wind at 500 m AGL. According to Weisman and Klemp (1986), storm type is often dependent on the value of the BRN. A decrease in BRN indicates that multicell convection has become better organized, and at small values supercell formation may occur. Greater values of the BRN are associated with multicell and air-mass thunderstorms. Table 2 shows some values of the BRN and their associated storm types.

Table 2: Values of the bulk Richardson number and associated storm types. Adapted from Weisman and Klemp, 1986.

BRN	Storm Type
~10-50	Supercell
~50-350	Multicell
>350	Air-mass

2.3.4 Precipitable water (PW)

Precipitable water (PW) is a measure of the total mass of water vapor in a column of air with 1 m^2 cross-sectional area (Djurić 1994). It quantifies the amount of water vapor that is potentially available for storm development. Precipitable water is given by

$$PW = \int_0^{\infty} q\rho \, dz = \frac{1}{g} \int_0^{p_0} q \, dp, \tag{2.8}$$

where q is the specific humidity, ρ is the density of moist air, and p_0 is the pressure at height $z = 0$. The specific humidity at a mandatory or significant pressure level, l, is found by

$$q_1 = \frac{\varepsilon e_l}{p_l}, \tag{2.9}$$

where e_l is the vapor pressure given by

$$e_l = 6.1e^{0.073 t_{dl}}, \tag{2.10}$$

and t_{dl} is the dewpoint temperature at mandatory or significant pressure level p_0 (Djurić 1994). The units of PW are in kilograms per meter squared but it is commonly expressed in millimeters of equivalent water depth (Dupilka and Reuter 2006b).

2.3.5 Storm convergence

It is suggested that in order for a tornado to form, vorticity would be enhanced by a rapid spin-up and simultaneous stretching of the vortex tubes which tends to increase the updraft velocity above cloud base. The

intensification of the low-level mesocyclone may be related to convergence at the base of the storm and thus be related to the potential for tornadogenesis (Lemon and Doswell 1979).

On the scale of which convection occurs, rate of change of vorticity is given by

$$\frac{d}{dt}(\zeta + f) = -(\zeta + f)\left(\frac{\partial u}{\partial x} + \frac{\partial v}{\partial y}\right) - \left(\frac{\partial w}{\partial x}\frac{\partial v}{\partial z} - \frac{\partial w}{\partial y}\frac{\partial u}{\partial z}\right) + \frac{1}{\rho^2}\left(\frac{\partial \rho}{\partial x}\frac{\partial p}{\partial y} - \frac{\partial \rho}{\partial y}\frac{\partial p}{\partial x}\right), \quad (2.11)$$

where (u,v,w) represent the wind components in Cartesian coordinates, vorticity $\zeta = \frac{\partial v}{\partial x} - \frac{\partial u}{\partial y}$, f is the Coriolis parameter, p is the perturbation pressure and ρ is the air density. Thus the rate of change of vorticity is given by the sum of the three terms on the right of equation 2.11 which are called the convergence term, the tilting term and the baroclinic term respectively (e.g. Holton 1979). These terms are also referred to as the vortex-stretching term, the twisting term and the baroclinic term (e.g. Holton 1979). According to Lemon and Doswell (1979), f is small compared to ζ on the convective timescale and can be neglected.

This study considers the case where the convergence, or vortex-stretching, term dominates as vorticity ζ increases in magnitude during the development of a low-level mesocyclone. Thus, when the tilting and baroclinic terms are neglected, equation 2.11 becomes

$$\frac{d\zeta}{dt} = \zeta\frac{\partial w}{\partial z} = \zeta C, \quad (2.12)$$

where the convergence, C, is given by

$$C = \frac{\partial w}{\partial z} = -\left(\frac{\partial u}{\partial x} + \frac{\partial v}{\partial y}\right). \tag{2.13}$$

In this equation, the quantity w represents the vertical updraft speed of the storm. Following Dupilka and Reuter (2006 b), convergence has been estimated using the proximity sounding via the equation

$$C = \frac{\partial w}{\partial z} \approx \frac{w(z_0 + \delta z) - w(z_0)}{\delta z}, \tag{2.14}$$

where $w(z)$ is the estimated storm updraft velocity as a function of height, z. The quantity z_0 describes the level of free convection (LFC), while δz denotes the vertical interval. The updraft velocity can be approximated by the equation

$$w(z+\delta z)^2 = w(z)^2 + 2g\int_z^{z+\delta z} \frac{T - T'}{T'}\, dz, \tag{2.15}$$

where T' and T represent the ambient and parcel temperatures respectively (e.g. Rogers and Yau 1996). In terms of CAPE, equation 2.15 becomes

$$w(z+\delta z)^2 = w(z)^2 + 2 \times CAPE, \tag{2.16}$$

where CAPE, or the thermal buoyancy, between the levels z and $z+\delta z$ is, by definition,

$$CAPE \equiv g\int_z^{z+\delta z} \frac{T - T'}{T'}\, dz. \tag{2.17}$$

Thus, the maximum storm convergence, C_{layer}, can be found by combining equations 2.14 and 2.16 for the layer z to $z+\delta z$ to give

$$C_{layer} \approx \frac{\sqrt{w(z)^2 + 2 \times CAPE} - w(z)}{\delta z}. \tag{2.18}$$

To find the average storm convergence through a height from z_0 to $z_0 + N\delta z$, the following sum is used

$$C = \left(\frac{1}{N}\right) \sum_{z=z_0}^{z_0+N\delta z} \frac{\sqrt{w(z)^2 + 2 \times CAPE} - w(z)}{\delta z}, \tag{2.19}$$

where z_0 is the LFC, N is the number of intervals, and $w(z_0) \approx 0$. Storm convergence can be determined for either a height interval, δz, or a pressure interval, δp, via the hydrostatic equation, $\delta p = -\rho g \, \delta z$ (Dupilka 2006). The determination of both w and $CAPE$ are based on basic parcel theory in which aerodynamic drag, ambient mixing, non-hydrostatic pressure perturbations and the weight of condensed water (water drag) are neglected. Including these contributions would likely reduce the value of w suggested by simple parcel theory. Thus, equation 2.15 is taken to be an estimate of the *maximum* updraft velocity, and equation 2.19 is an estimate of the *maximum* average storm convergence for a layer (Dupilka 2006).

Following Dupilka, for each proximity sounding the convergence profile $C = C(z)$ was calculated at 5-mb pressure intervals. The convergence was then averaged for two layers: from the LFC to 50 mb above the LFC, (referred to as C50), and the layer from the LFC to 100 mb above the LFC, (C100). The units of storm convergence are inverse-seconds.

2.4 Summary

Contained in this chapter is a description of the Ontario tornado dataset and an example of a sounding from Buffalo. The dataset suitable for the sounding

analysis in this thesis consists of 60 soundings, representing a total of 80 tornado cases, taken at 0000 UTC at Buffalo, New York from 1961 to 1996. A detailed list of the tornado events chosen for the study appears in appendix C. The chapter also contained a description of the sounding parameters used in this study and how they were computed. The main sounding parameters were: bulk and directional wind shear, CAPE and bulk Richardson number, precipitable water, and storm convergence. The next chapter contains the significance of these parameters, past research, and the results of the sounding analysis for southern Ontario.

CHAPTER THREE

Ontario Tornado Climatology of Sounding Parameters

This chapter contains a discussion of the significance of the sounding parameters introduced in chapter two, including past research. The results of the analysis for tornadic storms in southern Ontario are presented for each parameter. The aim of this chapter is to investigate whether there are any significant differences between the storm environments which support strong versus weak tornadic storms in southern Ontario. In particular, this chapter will focus on whether there are differences between the storm parameters introduced in chapter two: bulk and directional wind shear, CAPE, BRN, PW, and storm convergence.

3.1 Wind shear

As stated earlier, severe thunderstorms are associated with strong wind shear and veering of winds with height (Darkow and Fowler 1971). In shallow cumulus clouds that do not precipitate, wind shear serves to displace the main updraft away from the centre of maximum buoyancy, thus inhibiting their growth into mature thunderstorms. But for severe thunderstorms, strong wind shear acts to move precipitation away from the updraft, allowing for enhanced storm circulation since the updraft is no longer subject to the effects of precipitation drag (Byers and Braham 1949). In their study of composite hodographs for different thunderstorm types in Alberta, Chisholm and Resnick (1972) found that short-

lived, airmass thunderstorms occurred within weak shear environments, while multicell thunderstorms tended to develop within environments of strong, unidirectional wind shear. Supercell thunderstorms, on the other hand, occurred when strong directional shear was observed in the lowest 2 km. However, not all supercell thunderstorms form tornadoes. It is still unclear as to whether or not tornadoes form in shear environments that differ from those which support non-tornadic storms, and whether or not tornado intensity is influenced by the amount and character of wind shear.

Many past studies have investigated the nature of wind shear environments during tornadic storms. It has been suggested by Lemon and Doswell (1979) that the strength of winds in the mid and upper levels is associated with significant tornadoes. As stated previously, it has been suggested that the development of low-level mesocyclones can contribute to the formation of tornadoes (e.g. Rasmussen et al. 1994, Thompson et al. 2003). It has been shown via numerical modeling by Brooks et al. (1994) that the strength of the storm-relative mid-level winds helps to enhance and sustain low-level mesocyclones. Johns and Doswell (1992) hypothesized that low-level shear combined with deep-layer shear may generate mesocyclones.

Clearly wind shear, especially in the near ground layer, plays a significant role in tornadogenesis. Indeed, Colquhoun and Shepherd (1989) found that the magnitude of wind shear in the surface to 600 mb layer correlated with tornado F-scale intensity. Monteverdi et al. (2003), in their study of California thunderstorms, found that wind shear profiles were useful to forecasters for

discriminating between tornadic thunderstorms and severe thunderstorms which produced weak tornadoes or none at all. For their proximity sounding analysis for supercell environments obtained by the Rapid Update Cycle (RUC) experiment, Thompson et al. (2003) categorized severe storms into three groups: non-tornadic, weak tornadic (F1-F0), and significantly tornadic (F2-F5). They found that significantly tornadic versus non-tornadic events could be distinguished between by examining the 0-1 km vector shear magnitude, while the 0-6 km vector shear magnitude could only distinguish between supercells and non-supercells, and not tornadic versus non-tornadic storms. Another RUC-obtained proximity sounding analysis performed by Hammil and Church (2000) found that the 0-4 km mean shear magnitude could distinguish between non-supercell thunderstorms, supercell thunderstorms and tornadic thunderstorms, but had greater success in distinguishing between tornadoes and the other two types of thunderstorms. Rasmussen and Blanchard (1998), in their proximity sounding analysis for all non-zero CAPE soundings in the United States during the year 1992, also found that 0-4 km mean shear was useful for distinguishing between all three of the following storm categories: ordinary non-supercell thunderstorms, supercell thunderstorms and tornadic thunderstorms. In the proximity sounding analysis done for storms in Alberta between 1967 and 2000 by Dupilka and Reuter (2006a), it was found that bulk shear in both the 900-800 mb level and the 900-500 mb levels showed utility in distinguishing between strong and weak tornadoes, but showed marginal differences between non-tornadic severe thunderstorms and weak tornadoes. Discussing whether or not

shear environments in southern Ontario allow for distinguishing between strong tornadic (ST) and weak tornadic (WT) events is the aim of this section.

3.1.1 Bulk wind shear

Bulk wind shear was calculated for the layers from 900 mb to 800 mb, 900 mb to 700 mb, 900 mb to 600 mb and 900 mb to 500 mb for each sounding in the southern Ontario dataset. Figure 3.1 shows a box and whiskers plot for these levels which are labeled SHR8, SHR7, SHR6 and SHR5, for each tornado type WT (F0-F1 tornadoes) and ST (F2-F4 tornadoes). A box and whiskers plot depicts a statistical overview of a certain quantity. The grey boxes denote the 25^{th} to 75^{th} percentiles, and the median is indicated by the horizontal bar inside these so-called 50% boxes. The whiskers then depict the entire range of values. For the 900-800 mb layer, the median value for the ST case was 7.34 $m\ s^{-1}\ km^{-1}$, while the WT case was lower at 5.47 $m\ s^{-1}\ km^{-1}$. This was the only layer for which the medians differed by any significant amount and is also the layer which showed the largest range of values. This observation is consistent with the passing of fronts which typically possess strong temperature gradients. The other layers differed by only +0.19 $m\ s^{-1}\ km^{-1}$, -0.21 $m\ s^{-1}\ km^{-1}$ and -0.53 $m\ s^{-1}\ km^{-1}$ respectively, meaning for the two layers 900-700 mb and 900-600 mb the ST shear value was actually less than that of WT. For all four layers the 50% boxes showed significant overlap, and none of the 50% boxes were consistently separated for the ST and WT cases. Thus, the

conclusion is that bulk shear values did not distinguish strong from weak tornado events for tornadic storms in southern Ontario.

3.1.2 Directional wind shear

Also explained in chapter two, speed wind shear in addition to directional shear was calculated using a parameter called INIS, first introduced by Colquhoun and Shepherd (1989). Like bulk shear, INIS was calculated for the layers 900 mb to 800 mb, 900 mb to 700 mb, 900 mb to 600 mb and 900 mb to 500 mb for each sounding in the southern Ontario dataset. Figure 3.2 shows the box and whiskers plot depicting INIS values for southern Ontario dataset. The 900-800 mb layer had the largest range and was the only layer for which the median value was discernibly larger for the ST cases versus the WT cases, (5.00 $m\ s^{-1}\ km^{-1}$versus 3.16 $m\ s^{-1}\ km^{-1}$ respectively). Again, this observation is consistent with the vicinity of a baroclinic frontal zone which is characterized by a change in wind direction. The 900-600 mb and 900-500 mb layer also showed greater median values for the ST cases, but the difference was not very substantial, (+0.36 $m\ s^{-1}\ km^{-1}$ and 0.49 $m\ s^{-1}\ km^{-1}$ respectively). In contrast, the 900-700mb layer showed the WT median (2.51$m\ s^{-1}\ km^{-1}$) being greater than that of ST (2.71$m\ s^{-1}\ km^{-1}$). However, as with the bulk shear values, all of the 50% boxes showed significant overlap between both the ST and WT cases and none of the levels seemed to show any discernable separation. Therefore, INIS was not a useful parameter to clearly distinguish between storm types in southern Ontario.

3.2 CAPE

Along with wind shear, another atmospheric condition typically associated with severe thunderstorms is convective available potential energy (CAPE). CAPE quantifies the maximum vertical kinetic energy available to air parcels and is proportional to the square of maximum updraft speed. Since strong updrafts allow for the formation of hailstones, supercells and violent tornadoes, it seems logical to investigate CAPE as a parameter that might be useful for distinguishing between strong and weak tornadoes. As stated earlier, the method for measuring CAPE in this study is the most-unstable (MUCAPE) method which is based on the most unstable air parcel in the lowest 300 mb of the sounding. This method was chosen as it generally provides the maximum amount of CAPE (Doswell and Rasmussen 1994).

Many past studies have investigated the relationship between CAPE and severe weather. A study of 184 tornado proximity soundings compiled by the University of Missouri revealed that the direct relationship between CAPE and tornado intensity does not always hold (Kerr and Darkow 1996). A study of tornadic and non-tornadic mesocyclones by Brooks et al. (1994) also revealed that the amount of buoyant energy available does not always correlate with the intensity of severe storms. However, some studies have shown that CAPE values correlate rather well with storm intensity. Rasmussen and Blanchard (1998) showed that CAPE can distinguish quite well between ordinary severe thunderstorms and supercell or tornadic storms, but significant overlap is shown between tornadic and non-tornadic supercell thunderstorms. Thus, CAPE alone

is probably not a useful supercell predictor. Hamilll and Church (2000) achieved similar results. Thompson et al. (2003) used mean-layer CAPE (MLCAPE) in their study, which was found by raising a parcel from 100 mb above the surface. Their results also indicate the usefulness of CAPE to distinguish between non-tornadic severe thunderstorms and tornadic storms of all intensities, as well as an apparent ability to distinguish between the strong and weak tornadoes. However, it should be noted that the median values for these two tornadic storm types differ by a mere 300 J kg^{-1} (approx.) and that all storm categories show significant overlap (see Fig. 6 Thompson et al. (2003)). In contrast, the proximity sounding analysis performed on the Alberta dataset by Dupilka and Reuter (2006a) showed that MUCAPE as well as MLCAPE showed little utility for distinguishing between non-tornadic severe thunderstorms, weak tornadoes and significant tornadoes.

The aim of this section is to examine whether the total buoyant energy, quantified in the value MUCAPE, can distinguish between strong and weak tornadic storms in southern Ontario. Figure 3.3 shows a box and whiskers plot of MUCAPE values and compares them for strong and weak tornadoes. For this dataset, the 50% boxes showed large overlap and the median MUCAPE value was actually less for strong tornadic storms than for weak tornadic storms (313 J kg^{-1} versus 650 J kg^{-1} respectively). These CAPE values correspond to maximum updraft velocities of 25 ms^{-1} and 36 ms^{-1}, which correspond to maximum hail sizes of 3.8 cm (walnut) and 7.0 cm (baseball) (see Appendix D). Most strong tornadoes featured CAPE below 1000 J kg^{-1}, and some weak

tornadoes occurred in CAPE environments of 1000 J kg^{-1} or greater. Both categories showed a large range in values, but the weak tornado group showed the widest range overall which is consistent with the fact that this group contained the most storms. Thus, there appeared to be no trend between increasing MUCAPE values and increasing tornado intensity for southern Ontario. It should be noted, though, that MUCAPE values may not always be representative of the storm environment due to its sensitivity on the temperature and humidity sounding, properties which may vary substantially especially in the lower levels.

3.3 Combinations of shear and CAPE

Based on the studies mentioned above concerning wind shear and CAPE as predictor parameters on their own, more recent work has concentrated on parameters involving combinations of both wind shear and CAPE. It has been theorized by Rasmussen and Wilhelmson (1983) that tornadic storms tend to form in environments characterized by high wind shear (>3.5 x 10^{-3} $m\ s^{-1}\ km^{-1}$) and high CAPE (>2500 J kg^{-1}), while non-rotating, severe thunderstorms tend to form in environments with low shear and low CAPE. In contrast, though, Turcotte and Vigneux (1987) determined that high values of both shear and CAPE could not discriminate between non-tornadic severe thunderstorms and tornadic storms, as did Brooks et al. (1994). It has been theorized by Brooks et al. (1994) that because tornado formation tends to be associated with the development of a low-level mesocyclone, combinations of shear and CAPE may

not discriminate between storm types because low-levels (i.e., 1 km AGL) do not possess large values of CAPE. In their study of atmospheric soundings taken in near-tornado environments, Schaefer and Livingston (1988) found that pre-storm environmental conditions typically featured a balance between the strength of wind veering and the amount of atmospheric instability. They found that the strongest tornadoes occur when both veering and instability are strong while weaker tornadoes featured strong instability but weak winds.

The dependency of storm structure on the character of wind shear combined with CAPE was first examined by Weisman and Klemp (1982, 1984). They defined a parameter called the bulk Richardson number (BRN) which quantified this relationship, and it has been used as a supercell predictor since its inception. As explained in chapter two, a decrease in the BRN indicates that multicell convection has become better organized. When combined with a large CAPE, small values of the BRN (<50) indicate that supercell formation may occur, whereas greater values of the BRN are associated with multicell and air-mass thunderstorms. The usefulness of the BRN to discriminate between storm types was investigated by Thompson et al. (2003). When using the mean-layer CAPE (MLCAPE), they found that the BRN values discriminated rather well between non-supercells and supercells when focusing on the median values, since the range of the BRN for non-supercell thunderstorms was very large (10 to 627 at the 90^{th} percentile). Dupilka and Reuter (2006a) also investigated this parameter for their Alberta dataset. They calculated the BRN using MUCAPE and the 900-500 mb shear value rather than the shear difference between the

pressure-weighted mean wind from the surface to 6 km above ground level (AGL) and the wind at 500 m AGL as defined in chapter two. They found that this modified BRN does prove useful to discriminate strong tornadic storms from weak and non-tornadic storms. They found that the BRN was less useful than wind shear, but more useful than MUCAPE alone.

The current study of tornadic storms in southern Ontario also examined this parameter as a discriminator between storm types. Figure 3.4 shows a box and whiskers plot of BRN values and compares them for strong and weak tornadoes. For this dataset, the median value for strong tornadic storms was slightly larger than that of the weak tornadic storm category (14 versus 11 respectively). However, the 50% boxes generally overlapped indicating that the BRN offered little use for distinguishing between strong and weak tornadoes in southern Ontario. As was the case with MUCAPE, the weak tornado group showed the widest overall range of values which is again consistent with the fact that this group contained the most storms. For both storm categories, BRN values were below 50 up to the 75^{th} percentile indicating that many of these events may have been associated with supercell thunderstorms.

Along with the BRN, other parameters involving shear and CAPE have been examined in past research as well. One example is the energy-helicity index (EHI), a parameter which has been used operationally for supercell and tornado forecasting. Rasmussen and Blanchard (1998) examined this parameter in their proximity sounding analysis and found that it provided good discrimination between all three of the following storm categories: ordinary severe

thunderstorms, supercell thunderstorms and tornadic thunderstorms. Rasmussen (2003) revised this parameter in a later study to include helicity in the lowest 1 km. This modification substantially improved the discrimination between strong and weak tornadic supercells, but lessened the discrimination between non-tornadic severe thunderstorms and supercells. Similar results were found by Thompson et al. (2003) using Rasmussen's modified EHI and mean-layer CAPE (MLCAPE). Another example of a parameter involving both shear and CAPE is the vorticity generation parameter (VGP). It is meant to estimate the tilting and stretching rate of horizontal vorticity by a thunderstorm updraft. Investigation of this parameter by Rasmussen and Blanchard (1998) yielded similar results to EHI, but to a lesser degree. As with EHI, they found that the VGP was a good discriminator between all three categories of storm types and showed a definite difference between strong and weak tornadic supercells. Hamill and Church (2000) also analyzed this parameter and achieved similar results. Yet another example is the strong (or significant) tornado parameter. The strong tornado parameter was first introduced by Craven and Brooks (2004). It consists of a combination of parameters including both shear and CAPE and is based on the significant tornado parameter (Thompson et. al 2003) which uses helicity in the lowest kilometer rather than the bulk shear value. The strong tornado parameter showed utility in distinguishing between significant tornadoes and significant wind/hail events (Craven and Brooks 2004) as did the significant tornado parameter in distinguishing between significant tornadoes, weak tornadoes, and non-tornadic supercell thunderstorms (Thompson et al. 2003).

These and other past studies (Maddox 1976 and Johns and Doswell 1992) seem to suggest that tornadoes form within a broad range of shear and CAPE environments. It is likely a combination of physical processes that combine to promote tornadogenesis, and these processes may (or may not) occur in environments represented by the parameters that are chosen to be studied. Thus, high threshold values of both shear and CAPE should not be solely relied upon to forecast the probability of tornadic development and subsequent tornado intensity.

3.4 Precipitable water

As explained in chapter one, it has been suggested that the initial development of rotation in a low-level mesocyclone may depend on the initial formation of a rain-cooled downdraft located in the rear-flank of a supercell (Rotunno and Klemp 1985, Klemp 1987, Davies-Jones and Brooks 1993 and Markowski et al. 2002). Brooks et al. (1994) suggest that the amount of water vapor in the storm environment should affect the amount of precipitation generated, which would then influence the downward buoyancy caused by evaporative cooling of rain. This is significant because the downward buoyancy located in the rear-flank downdraft (RFD) may be what generates vorticity (Lemon and Doswell 1979). It is thought that greater atmospheric moisture content may assist in strengthening and maintaining the RFD by allowing the mesocyclone to transport more rain to its rear flank. Numerical simulations performed by Markowski et al. (2002) have investigated how thermodynamic

differences within the RFD can influence tornado formation. They found that supercells containing RFDs with relatively small temperature deficits tend to produce tornadoes more often than supercells containing RFDs with relatively large temperature deficits. Smaller temperature deficits are associated with higher relative humidities, and as the deficit decreases buoyancy of air parcels in the downdraft (and resulting convergence of angular momentum) increases, creating more intense and longer lived tornadoes since warm air parcels tend to accelerate rapidly upward as they approach the axis of rotation (Markowski et al. 2002). Thus it seems that greater moisture in the atmosphere may contribute to the formation of more intense, longer lasting tornadoes. As stated in chapter two, a parameter useful for quantifying the amount of water vapor in the atmosphere is precipitable water (PW), which is expressed in millimeters of equivalent water depth.

The vertical distribution of water vapor clearly seems to have a significant impact on storm development. However, it has shown by Ross and Elliot (1996), Wittmeyer and Vonder Haar (1994) and Djurić (1994) that PW values might be regional. Through radiosonde observations over a twenty year period from 1973 to 1993, Ross and Elliot (1996) showed that regions of the south-central United States have annual PW values between 20 and 30 mm, whereas areas in the high-altitude west have annual averages as little as 10 mm. The average PW for Alberta was shown to be approximately 15 mm, and for southern Ontario it was approximately 18 mm. By using satellite observations for a six year period from 1983 to 1989, Wittmeyer and Vonder Haar (1994) showed similar results.

According to Djurić (1994), convection in the south-central United States is typically associated with PW values of approximately 25 mm, whereas convection in the high plains can occur with PW values as little as 10 mm. In their evaluation of PW for convective storms in Alberta, Dupilka and Reuter (2006b) found that severe thunderstorms and tornadoes occurred when PW values were in excess of 20 mm, a rarity in Alberta (Taylor 1999). This study is concerned with finding the PW values associated with tornadic thunderstorm events in southern Ontario.

The PW for each case in the study is shown in Figure 3.5. The median value was 34 mm for the ST category and 28 mm for the WT category, indicating greater separation than any other parameter thus far. For all cases, the 50% boxes covered a range from 21-43 mm, with the strong tornadoes encompassing the 27-43 mm range, and the weak tornadoes encompassing the 21-34 mm range. Thus, strong tornadoes occurred when the atmosphere was generally moist with 75% of them occurring when the PW is over 27 mm. In the weak tornado category, 75% of storms occurred when the PW was over 21 mm. This seems to suggest that most tornadoes in Ontario develop when the precipitable water is 20 mm or greater.

3.5 Storm convergence

The expression for storm convergence was introduced in chapter two. Equation 2.11 describes the evolution of vorticity as being the sum of three terms: a convergence term, a tilting term and a baroclinic term. (Or, alternatively,

a vortex-stretching term, a twisting term, and a solenoidal term). It is thought that in order for a tornado to form, the low-level horizontal vorticity would first be tilted into the vertical, and the vertical vorticity would be amplified through vortex stretching. Thus, the tilting (or twisting) term is likely the dominant contributor in the vorticity equation, with the convergence (or vortex-stretching) term at near its strength, especially at low levels (Lemon and Doswell 1979). Indeed, studies conducted by both Doswell and Bluestein (2002) and Zeigler et al. (2001) concluded that the formation of a low-level mesocyclone was preceded by the tilting of horizontal vorticity into the vertical, followed by a period of intense stretching of vertical vorticity. A typical mesocyclone has a radius of approximately 5 km and a vorticity on the order of 0.01 s^{-1}. In order for a tornado to form, the vorticity must increase by approximately 100 times to 1.0 s^{-1} while its radius decreases to approximately 100 m. It seems logical that the rapid spin-up of vorticity necessary for tornado formation is related to convergence at the storm base (e.g. Lemon and Doswell 1979).

As stated in chapter two, this study is concerned with the case where the convergence term is dominant, and the tilting and baroclinic terms are neglected. In this case, the expression for convergence is given by equation 2.14. Again, the storm convergence was calculated for two layers: 50 mb above the level of free convection (LFC) (C50) and 100 mb above the LFC (C100). Dupilka and Reuter (2006b) calculated storm convergence for the same two layers in their evaluation of Alberta convective storms. Their results suggest that storm convergence above the LFC does not discriminate among the storm categories

for severe convective events in Alberta. Figures 3.6a and 3.6b show the storm convergence profiles for strong and weak tornadoes in southern Ontario. For the C50 layer in Figure 3.6a, the medians were similar at 10.0 x 10^{-3} s^{-1} for the strong tornado category, and 10.6 x 10^{-3} s^{-1} for the weak tornado category. Also, the 50% boxes showed complete overlap and offered no discernable discrimination between storm types. Figure 3.6b shows similar results for the C100 layer. The medians were 9.1 x 10^{-3} s^{-1} and 8.8 x 10^{-3} s^{-1} respectively with the 50% boxes again showing no discernable discrimination between storm category. It is interesting to note that for the C50 layer, the WT category has a median value which is marginally higher than the ST category, while for the C100 layer the opposite is true. Thus it seems that storm convergence is not a good parameter to discriminate between strong and weak tornadic storms in southern Ontario.

3.6 Summary

The aim of this chapter was to investigate whether there are any differences in the storm environments which support strong versus weak tornadic storms in southern Ontario. For the parameters involving wind shear, it was found that neither bulk shear nor directional shear offer any help in distinguishing between tornado categories. It was also found that there was no trend between increasing CAPE values and increasing tornado intensity. The bulk Richardson number, a combination of shear and CAPE, also offers no discernable discrimination between storm categories.

Precipitable water, however, does show some assistance in distinguishing between storm categories, suggesting that strong tornadoes in southern Ontario tend to occur when the atmosphere is especially moist. The parameter storm convergence did not offer any skill in distinguishing between storm types for either the layer 50 mb above the LFC (C50) nor the layer 100 mb above the LFC (C100). The next chapter will compare these results to some parameters contained in the sounding analysis for Alberta completed by Dupilka and Reuter (2006a, b).

CHAPTER FOUR

Comparison Between Sounding Climatologies of Alberta and Ontario

This chapter compares the results for tornadic storms in Ontario to results for tornadic storms in Alberta (Dupilka and Reuter 2006a, b). It begins with a detailed discussion about the differences and similarities in the databases for southern Ontario and central Alberta. The focus of this chapter is on determining if there are any differences between the soundings supporting strong versus weak tornadic storms for the two provinces. In particular, this chapter will concentrate on any differences in magnitude and range of bulk wind shear, CAPE, precipitable water and storm convergence.

4.1 Data selection and database

Both the Alberta and Ontario sounding climatology studies are very similar in many ways, but there are a few differences in the way the data was selected. All information regarding the Alberta study is taken from Dupilka and Reuter (2006a, b).

The Alberta study concentrated on the area surrounding the Stony Plain (WSE) upper-air station in north-central Alberta. The dataset consisted of 87 storm events occurring from 1967-2000, 74 of which were tornadic and 13 of which were non-tornadic severe thunderstorms which produced hail sizes of at least 3 cm. In contrast, the Ontario dataset centered around Buffalo, New York (BUF) and consisted of only tornadic storms which occurred between 1961 and

1996. There were 60 storm soundings in this dataset. The Alberta data came from two sources. For events prior to 1985, the data were taken from Hage's (2003) dataset of Canadian prairie windstorms, and for events after 1985, the data were taken from the Severe Storm Archive of Environment Canada. For the Ontario study, all of the data came from this same archive. In both cases, storm events that occurred prior to the earliest year in the study (1967 and 1961 respectively) were not included because neither upper-air station produced soundings before these dates. In both studies, if separate locations in close proximity reported the occurrence of a tornado, it was assumed to be sightings of the same tornado and was taken to be a single event. For such instances, the location at which the greatest damage occurred was used for the F-scale damage rating. Also, when multiple tornado events occurred on the same day, the highest F-scale rating was chosen and the representative sounding was used only once in the dataset.

In Alberta, storm events that occurred within a 200 km radius of the Stony Plain upper-air station were selected for the dataset. This criterion successfully captured most of the strong tornado events ($\geq$ F2). In Ontario, however, this criterion would have only captured 43 tornadic events, only four of which were F2 or greater in strength. Thus, in order to increase the number of soundings in the study, Rasmussen and Blanchard's (1994) *boundary layer wind vector* criteria was used for events that occurred between 200 and 300 km from BUF (see figure 1 in Rasmussen and Blanchard 1998). By using this method, the strong tornado category increased from four events to ten, and the weak tornado

category increased from 39 to 50, allowing for an additional 17 soundings to be included in the study, meaning the total number was increased to 60 (see Appendix C). This example illustrates how difficult it is to achieve a reasonably sized dataset of what are essentially rare events.

In both studies, the 0000 UTC sounding corresponding to the day of the tornado event was selected for analysis. This corresponds to 1800 local time in Alberta and 2000 local time in Ontario. The Hage dataset (pre-1985 for Alberta storms) does not record the time that events occurred, but from the Environment Canada dataset, the mean time for Alberta storms with hail $\geq$ 1 cm is 2350 UTC with approximately 93% occurring within $\pm$ six hours of 1800 local time. For Ontario, the mean time for all tornadic storms included in the Environment Canada dataset was 1743 local time. Thus the choice to use the 0000 UTC sounding was reasonable for both studies. Smaller constraints in time and space may provide better proximity soundings, but the sizes of the datasets would have decreased significantly as a result.

Both The Ontario and the Alberta datasets were inspected using the RAOB software package. For each sounding, RAOB was used to determine the most-unstable CAPE. If the MUCAPE was below 50 J kg^{-1}, the sounding was rejected in both studies. This constraint was used in order to eliminate soundings that may be associated with microbursts. All of these restrictions resulted in 87 storm soundings for the Alberta dataset, 74 of which were tornadic and 13 of which were non-tornadic storms with hail size $\geq$ 3 cm, and 60 soundings for the Ontario dataset, all of which were associated with tornadic

storm events. For Alberta, the restrictions eliminated 30 tornadic events and one non-tornadic event, whereas for Ontario, the restrictions eliminated 131 tornadic events.

The frequency of tornado occurrence versus F-scale is compared for Alberta and Ontario in Figure 4.1. According to Etkin (2001), 22% of Canadian tornadoes occur in Alberta whereas 32% occur in Ontario. In both provinces, the overall distribution of tornado strength is similar, however Alberta generally experiences more F0 tornadoes and less F1 tornadoes than Ontario. There has not been a documented case of an F5 tornado in either province. When separated into the strong (F4, F3 and F2) and weak (F1 and F0) tornado categories, the Alberta dataset divides into 18% strong and 82% weak, which is comparable to Ontario's distribution of 17% strong and 83% weak. Both provinces have a similar frequency to all of Canada which experiences 18% strong and 82% weak tornadoes.

4.2 Bulk wind shear

The focus of this section is to compare the sounding climatology profiles of Alberta and Ontario for bulk wind shear. Figure 4.2 shows two box and whiskers plots depicting bulk shear values for Alberta (top) and Ontario (bottom). At a first glance, comparison of the ST and WT cases depicts that the Alberta dataset showed better discrimination between categories than did the Ontario dataset. For all four layers of shear in the Alberta data, the median values were consistently larger for the ST cases than for the WT cases. The 50% boxes

showed a similar finding in that the ST cases showed little overlap with the WT cases and the boxes depicting WT cases were consistently lower. In contrast, the only layer that showed any discernable difference in median for the Ontario dataset was the 900-800 mb layer. All of the other layers differed very little in median value and all 50% boxes showed significant overlap. In the 900-700 mb and 900-600 mb layers, the ST value was actually smaller than the WT value. In both cases, the 900-800 mb layer showed the greatest range in values which is again consistent with the passage of fronts which are typically characterized by strong temperature gradients.

Overall, bulk shear provided greater separation among storm categories for Alberta storms than for Ontario.

4.3 CAPE

This section focuses on comparing the amount of available buoyant energy for both provinces. Figure 4.3 shows two box and whiskers plots portraying MUCAPE for Alberta (top) and Ontario (bottom). For the Alberta dataset, the ST events had a median value of about 1050 J kg^{-1} which was slightly larger than the WT median value which was approximately 900 J kg^{-1}. Both categories showed a large range of MUCAPE values and the 50% boxes showed significant overlap. For the Ontario data, the median values and the 50% boxes were consistently lower than those for Alberta. In fact, for Ontario the median for ST was actually less than that of WT and the maximum value for ST was also comparatively low. Generally, the Alberta dataset had greater

MUCAPE values for both storm categories. This suggests that Alberta is more atmospherically unstable than Ontario and also encounters greater hail sizes due to higher updraft velocities.

4.4 Precipitable water

The aim of this section is to compare atmospheric moisture profiles for Alberta and Ontario by examining precipitable water (PW) values. Figure 4.4 displays PW values for Alberta (top) and Ontario (bottom). For the Alberta dataset, the PW values had a relatively narrow range from about 20 mm to 30 mm. The median values showed some separation between categories and were 25 mm for ST and 22 mm the WT. The 50% boxes showed some overlap but the ST values were generally greater than the WT values. This finding was also apparent for Ontario.

PW values were generally higher for Ontario tornadic storms compared to Alberta tornadic storms. However, throughout the year the atmosphere over southern Ontario tends to contain more moisture compared to the atmosphere over central Alberta. Satellite and radiosonde observations (Wittmeyer and Vonder Haar 1994, Ross and Elliot 1996) have indicated that the average annual PW value for Alberta is approximately 15 mm and for southern Ontario it is slightly greater at 18 mm. From Figure 4.4 it does seem, though, that typical storm environments tend to be more humid in southern Ontario in comparison to storm environments over central Alberta.

4.5 Storm convergence

Storm convergence is compared for Alberta and Ontario in Figures 4.5a and 4.5b. Figure 4.5a depicts storm convergence values for the layer 50 mb above the LFC (C50) and Figure 4.5b depicts the 100 mb above the LFC layer. Again, the Alberta data is presented in the top box and whiskers plot in both figures.

For the Alberta data, the C50 median values (Figure 4.5a) for the ST and WT categories were similar at about 10 x 10^{-3} s^{-1}. The 50% boxes showed almost complete overlap and offered no discernable differences between storm categories. For both tornado categories the 50% box ranged from about 9 x 10^{-3} s^{-1} to 12 x 10^{-3} s^{-1}. The Ontario dataset yielded identical results.

For the C100 layer in Figure 4.5b, the 50% boxes for both provinces again showed significant overlap. The Alberta medians for the WT and ST cases were approximately 9 x 10^{-3} s^{-1} and the 50% box ranged from about 7 x 10^{-3} s^{-1} to 11 x 10^{-3} s^{-1} for both categories and again the Ontario data yielded identical results. Thus it is apparent that storm convergence above the LFC is not a helpful discriminator to distinguish between strong and weak tornadoes in either Alberta or Ontario.

4.6 Parameter threshold pairs

As described in section 4.2, the Alberta data indicated that the 900-800 mb layer (SHR8) and the 900-500 mb layer (SHR5) offered some usefulness for discriminating among ST and WT. Similarly, section 4.4 noted that PW was also

a useful parameter for discriminating among storm types. This suggests that a pair of shear values may be more useful than any of these parameters alone. Thus, threshold pairs were investigated between SHR5 and SHR8 and between PW and SHR5 to assess the potential for storms to become significantly tornadic. This section is devoted to comparing threshold pairs for the Alberta and Ontario datasets.

Figure 4.6 shows scatter plots of SHR8 versus SHR5 values for Alberta (top) and Ontario (bottom). For the Alberta data, non-tornadic severe thunderstorms with hail size of at least 3 cm are denoted by solid diamonds. In both figures, WT are denoted by open squares and ST are denoted by open circles. The top figure (Alberta) shows two quadrants: one generated by the threshold pair SHR5 = 3 $m\ s^{-1}\ km^{-1}$ and SHR 8 = 6 $m\ s^{-1}\ km^{-1}$ (solid line) and another generated by SHR5 = 3 $m\ s^{-1}\ km^{-1}$ and SHR8 = 0 $m\ s^{-1}\ km^{-1}$ (dashed line). The solid line indicates that 77% of ST events occurred within this quadrant while only 18% of WT events occurred here. This suggests that the threshold pair SHR5 = 3 $m\ s^{-1}\ km^{-1}$ and SHR 8 = 6 $m\ s^{-1}\ km^{-1}$ offers some skill in predicting the likelihood of ST versus WT in Alberta. The dashed line increases the ST occurrence to 100%, but 34% of WT cases also occurred here, meaning the false alarm rate for forecasting ST events versus WT events increases as well. The bottom figure (Ontario) did not offer any such threshold pair since both the strong tornadoes (solid circles) and weak tornadoes (open squares) were scattered across the whole range of SHR5 and SHR8 values. This is consistent with the fact that SHR5 and SHR8 offered no discernable

discrimination between ST and WT for the Ontario dataset while for the Alberta dataset they did.

Figure 4.7 shows a scatter plot of PW versus SHR5 values for Alberta (top) and Ontario (bottom). In the same way as Figure 4.7, two quadrants are generated by the threshold pairs SHR5 = 3 $m\ s^{-1}\ km^{-1}$, PW = 23 mm and SHR5 = 3 $m\ s^{-1}\ km^{-1}$, PW = 21 mm indicated by the solid and dashed lines respectively. The solid line encompasses 77% of ST cases and 20% of WT cases, and the dashed line encompasses 100% of ST cases and 25% of WT. These data suggest that the threshold pair SHR5 = 3 $m\ s^{-1}\ km^{-1}$ and PW = 23 mm may offer some skill in assessing the likelihood of ST versus WT in Alberta. Although PW did discriminate among storm categories for the Ontario dataset, the bottom scatter plot of PW and SHR5 (Ontario) offered no discernable threshold pair since both strong and weak tornadoes occurred across the whole range of SHR5 values. Thus creating threshold pairs between SHR5 and SHR8 and between PW and SHR5 was useful for assessing the potential of strong versus weak tornadoes in Alberta, but was not useful for Ontario.

4.7 Summary

This chapter contained a comparison between the results for tornadic storms in Ontario versus the results for tornadic storms in Alberta obtained by Dupilka and Reuter (2006a, b). The goal of this chapter was to determine if there were any differences between the environmental soundings supporting strong versus weak tornadic storms in southern Ontario and central Alberta.

The Alberta dataset consisted of 74 tornado event soundings whereas the Ontario dataset contained 60. The frequency of tornado occurrence versus F-scale was similar for both provinces and also similar to the distribution for the whole of Canada. Following this discussion was a comparison of bulk wind shear between the two studies. It was found that bulk shear provided some separation among storm categories for Alberta, but this distinction was not apparent for Ontario. The investigation of CAPE values for both studies showed no trend between increasing CAPE and increasing tornado intensity, but the comparison suggests that Alberta is more atmospherically unstable than Ontario and also encounters greater hail sizes due to higher updraft velocities, i.e. generally higher CAPE values. The precipitable water (PW) comparison yielded similar results for both provinces. Generally, strong tornadoes tended to occur in atmospheres that had higher PW values, i.e., atmospheres that were exceedingly humid. The PW values suggest that typical tornadic storms in southern Ontario tend to be formed in more humid air masses than tornadic storms forming over Alberta. However, research suggests that the average annual precipitable water is greater in the Ontario region that it is in Alberta. For the storm convergence parameter, neither study suggested that it was a useful discriminator between strong and weak tornadic storms.

The Alberta study investigated threshold pairs between SHR5 and SHR8 as well as PW and SHR5. It was thought that because each of these parameters offered some ability to distinguish between strong and weak tornadic storms, perhaps a pair of values would be more useful than any parameter alone.

Similar two-parameter plots were computed for the Ontario tornadic storms dataset. It was found that creating threshold pairs between SHR5 and SHR8 and between PW and SHR5 was useful for assessing the potential of strong tornadoes versus weak tornadoes in Alberta, but this discrimination was not apparent for Ontario.

CHAPTER FIVE

Conclusions and Discussion

This final chapter contains a summary of the results and a discussion on the importance of the research findings. The chapter will conclude with some suggestions for further research.

5.1 Conclusion

This thesis investigated the use of radiosonde data to assist in forecasting the likely intensity of tornadic storms in southern Ontario. Specifically, it investigated whether there are differences between sounding environments of strong (F2, F3 and F4) and weak (F0 and F1) tornadic storms in Ontario. It also addressed whether there are differences between the soundings supporting strong versus weak tornadic storms in southern Ontario and central Alberta. The dataset consisted of 80 tornado events in southern Ontario which were represented by 60 soundings, ten of which were associated with strong tornadoes and fifty associated with weak tornadoes. The soundings in the Ontario study were taken at 0000 UTC from Buffalo, New York (BUF). The parameters investigated included bulk and directional wind shear for different pressure layers, convective available potential energy (CAPE), the bulk Richardson number (BRN), which is a combination of shear and CAPE, precipitable water (PW), and storm convergence, a parameter first introduced by Dupilka and Reuter (2006b).

For tornadic storms in southern Ontario, it was found that parameters involving wind shear offered no discernable discrimination between strong and weak tornadic storms. It was also found that increasing CAPE values were not accompanied by increasing tornado intensity. In fact, the median CAPE value for strong tornadoes was slightly less than that of weak tornadoes. The bulk Richardson number, a combination of shear and CAPE, also offered no assistance in discriminating between tornadic storm types in southern Ontario. Precipitable water, however, did offer some ability to distinguish between storm categories, suggesting that tornadoes in southern Ontario tended to occur when the atmosphere is unusually humid. The storm convergence parameter also did not show any discernable difference between strong and weak tornadoes, for neither the 50 mb above LFC layer nor the 100 mb above LFC layer. Therefore, this research suggests that there are no differences between the sounding environments of strong and weak tornadic storms in southern Ontario, save for the fact that strong tornadoes tended to occur when the atmosphere is increasingly moist.

In comparing the Ontario sounding analysis and the previous Alberta sounding analysis completed by Dupilka and Reuter (2006a, b), it was found that bulk shear provided some separation among tornado categories in Alberta, but this distinction was not apparent for Ontario. The comparison of CAPE values revealed that neither study showed a trend between increasing CAPE and increasing tornado intensity. However, the Alberta CAPE values were consistently larger than the values for Ontario, suggesting that the atmosphere in

Alberta tends to be more unstable and allows for greater hail sizes due to higher updraft velocities. The precipitable water comparison yielded similar results in both studies in that strong tornadoes tended to occur in environments characterized by higher moisture content. Also, the precipitable water values were consistently larger in Ontario than Alberta suggesting that typical storm environments in Ontario contain more atmospheric moisture than those in Alberta. This correlates with the fact that annual average precipitable water values in Ontario are larger than they are in Alberta. For the storm convergence parameter, neither study suggested that it was a useful parameter for distinguishing among tornado types. In fact, the storm convergence values for both studies were nearly identical. The Alberta study investigated threshold pairs between SHR5 and SHR8, as well as PW and SHR5, since each of these parameters offered some probabilistic skill in discriminating among strong and weak tornadoes on their own. The thought was that there might be pairs of sounding parameter values which may offer more usefulness for discriminating among categories than any parameter alone was investigated. Thus, the same type of two-parameter plots were constructed for the Ontario dataset and compared with those constructed for Alberta. It was found that threshold pairs between SHR5 and SHR8 and between PW and SHR5 were useful for assessing the potential of strong tornadoes versus weak tornadoes in Alberta, but the same was not apparent for tornadic storms in southern Ontario.

5.2 Suggestions for further research

According to Moran (2006), over three quarters of tornadoes that occur are weak (F0 or F1), but they account for only 5% of fatalities. Thus it is the strong tornadoes (F2 and greater) that cause the vast majority of deaths associated with these violent storms. It seems useful, then, to be able to determine under which conditions strong tornadoes will occur versus weak. In an area of such high population density and high tornado occurrence as southern Ontario, making this distinction would serve to reinforce public safety and allow for emergency response to be on alert to take appropriate action should a severe tornado outbreak occur. This study found no discernable differences in storm environments as indicated by observed proximity soundings supporting strong versus weak tornadic storms in southern Ontario. However, it might be possible to discriminate between tornadic and non-tornadic storms. If this is feasible, it might yield useful information on whether or not tornadoes of any intensity were imminent in this region. Furthermore, this research could be extended to examine sounding parameters in regions with a similar climatology to Ontario such as areas in the United States where there exists a huge archive of severe storm data assembled by the Storm Prediction Center (SPC) of NOAA. This research could also be expanded to examine tornadoes for all regions across Canada.

References

Auld H., D. MacIver, J. Klaassen, N. Comer, and B. Tugwood, 2004: Atmospheric Hazards in Ontario, ACSD Science Assessment Series No. 3. Meteorological Service of Canada, Environment Canada, Toronto, Ontario, 72 p.

Brooks, H., E., C. A. Doswell III, and J. Cooper, 1994: On the environment of tornadic and non-tornadic mesocyclones. *Wea. Forecasting*, 9: 606-618.

Brooks, H. E., and C. A. Doswell III, 2001: Some aspects of the international climatology of tornadoes by damage classification. *Atmos. Res.*, 56: 191-202.

Brooks, H. E., R. B. Wilhelmson, 1994: The role of midtropospheric winds in the evolution and maintenance of low-level mesocyclones. *Mon. Wea. Rev.*, 122, 126-136.

Byers, H. R., and R. R. Braham Jr., 1949: *The Thunderstorm*. U.S. Government Printing Office, 287 p.

Chisholm, A. J., and J. H. Renick, 1972: The kinematics of multicell and supercell Alberta hailstorms. Research Council of Alberta Hail Studies Rep. 72-2, 7 p.

Colquhoun, J. R., and D. J. Shepherd, 1989: An objective basis for forecasting tornado intensity. *Wea. Forecasting*, 4: 35-50.

Craven, J. P., and H. E. Brooks, 2004: Baseline climatology of sounding derived parameters associated with deep, moist convection. *Natl. Wea. Dig.*, 28, 13-

24.

Darkow, G. L., and M. G. Fowler, 1971: Tornado proximity wind sounding analysis. Preprints, *7th Conf. on Severe Local Storms*, Kansas City, Missouri, Amer. Meteor. Soc., 148-151.

Davies, J. M., 2004: Estimations of CIN and LFC associated with tornadic and nontornadic supercells. *Wea. Forecasting*, 19: 714-726.

Davies-Jones, R. P., 1984: Streamwise vorticity: The origin of updraft rotation in supercell storms. *J. Atmos. Sci.*, 41: 2991-3006.

Davies-Jones, R. P., and H. E. Brooks, 1993: Mesocyclogenesis from a theoretical perspective. The Tornado: Its Structure, Dynamics, Prediction and Hazards. Geophys. Monogr., No. 79, Amer. Geophys. Union, 105-114.

Djurić, D. 1994: *Weather Analysis*. Prentice Hall Inc., 304 p.

Doswell, C. A. III, and H. B. Bluestein, 2002: The 8 June 1995 McLean, Texas storm. Part I: Observation of cyclic tornadogenesis. *Mon. Wea. Rev.*, 130, 2626-2648.

Doswell, C. A., III, and E. N. Rasmussen, 1994: The effect of neglecting the virtual temperature correction on CAPE calculations. *Wea. Forecasting*, 9: 625-629.

Dupilka, M. L., 2006: On forecasting severe storms in Alberta using

environmental sounding data. PhD thesis, University of Alberta, Edmonton.

Dupilka, M. L., and G. W. Reuter, 2006a: Forecasting tornadic thunderstorm potential in Alberta using environmental sounding data. Part I: Shear and buoyancy. *Wea. Forecasting*, 21: 325-335.

Dupilka, M. L., and G. W. Reuter, 2006b: Forecasting tornadic thunderstorm potential in Alberta using environmental sounding data. Part II: Helicity, precipitable water, and storm convergence. *Wea. Forecasting*, 21: 336-346.

Etkin, D., S. E. Brun, A. Shabbar, and P. Joe, 2001: Tornado climatology of Canada revisited: Tornado activity during difference phases of ENSO. *Int. J. Climatol.*, 21: 915-938.

Fujita, T. T., 1981: Tornadoes and downbursts in the context of generalized planetary scales. *J. Atmos. Sci.*, 38: 1511-1534.

Hamill, T.M., and A. T. Church, 2000: Conditional probabilities of significant tornadoes from RUC-2 Forecasts. *Wea. Forecasting*, 15: 461-475.

Holton, J. R., 1979: *An Introduction to Dynamic Meteorology*. 2nd ed. Academic Press, New York, New York, 300 p.

Hopkins, E. J., 1996: *Radiosondes – An upper air probe*. Retrieved March 9, 2008, from The University of Wisconsin, Madison, Department of Atmospheric and Oceanic Sciences Department Web site: http://www.meteor.wisc.edu/~hopkins/wx-inst/wxi-raob.htm

Iribarne, J. V., and Godson, W. L., 1981: *Atmospheric Thermodynamics*. 2nd edition. D. Reidel Publishing Company, Dordrecht, the Netherlands, 278 p.

Johns, R. H., and C. A. Doswell III, 1992: Severe local storms forecasting. *Wea. Forecasting*, 7, 588-612.

Kerr, B. W., and G. L. Darkow, 1996: Storm-relative winds and helicity in the tornadic thunderstorm environment. *Wea. Forecasting*, 11, 489-505.

Klemp, J. B., 1987: Dynamics of tornadic thunderstorms. *Annu. Rev. Fluid Mech.*, 19: 369-402.

Klemp, J. B., and R. B. Wilhelmson, 1978: The simulation of three-dimensional convective storm dynamics. *J. Atmos. Sci.*, 35: 1097-1110.

Lemon, L.R., and C. A. Doswell, 1979: Severe thunderstorm evolution and mesocyclone structure as related to tornadogenesis. *Mon. Wea. Rev.*, 107: 1184-1197.

Markowski, P. M., J. M. Straka, E. N. Rasmussen, 2002: Direct surface thermodynamic observations within the rear-flank downdrafts of nontornadic and tornadic supercells. *Mon. Wea. Rev.*, 130, 1692-1721.

Monteverdi, J. P., C. A. Doswell III, and G.S. Lipari, 2003: Shear parameter thresholds for forecasting tornadic thunderstorms in Northern and Central California. *Wea. Forecasting*, 18: 357-370.

Moran, J. M., 2006: *Weather Studies*. 3rd ed. American Meteorological Society, Boston, Massachusetts, 516 p.

The National Center for Atmospheric Research, 2005: *RAP Real-time weather data*. Retrieved February 23, 2008. from: http://www.rap.ucar.edu/weather/upper/

National Renewable Energy Laboratory, 2007: *Radiosonde / Weather Balloon Observations*. Retrieved March 9, 2008, from: http://www.srh.noaa.gov/mob/balloon.shtml

National Weather Service Southern Region Headquarters, 2008: *Skywarn Hail Comparison Chart*. Retrieved July 26, 2008, from: http://www.srh.noaa.gov/tbw/html/tbw/skywarn/hail.htm

Newark, M. J., 1984: Canadian tornadoes, 1950-1979. *Atmos. Ocean*, 22: 343-353.

Orf, L., and Wilhelmson, R., 2004: Evolution of tornado-like vortices in a numerically simulated supercell thunderstorm. Preprints, 22nd *Conf. on Severe Local Storms*, Hyannis, Massachusetts, Amer., Meteor. Soc., CD-ROM, 9.5.

Rasmussen, E. N., 2003: Refined supercell and tornado forecast parameters. *Wea. Forecasting*, 18, 530-535.

Rasmussen, E. N., and D. O. Blanchard, 1998: A baseline climatology of sounding-derived supercell and tornado forecast parameters. *Wea. Forecasting*, 13: 1148-1164.

Rasmussen, E. N., R. Davies-Jones, C. A. Doswell III, F. H. Carr, M. D. Eilts, D. R. MacGorman, J. M. Straka, and F. H. Carr, 1994: Verification of the Origins of Rotation in Tornadoes Experiment: VORTEX. *Bull. Amer. Met. Soc.*, 75: 995-1006.

Rasmussen, E. N., and R. B. Wilhelmson, 1983: Relationships between storm characteristics and 1200 GMT hodographs, low level shear and stability. Preprints, *13th Conf. on Severe Local Storms*, Tulsa, Oklahoma, Amer. Meteor. Soc., 55-58.

Rogers R. R., and M. K. Yau, 1996: *A short course in cloud physics*. 3rd edition. Butterworth-Heinemann, Woburn, Massachusetts, 290 p.

Ross, R. J., and W. P. Elliot, 1996: Tropospheric water vapor climatology and trends over North America: 1973-1993. *J. Climate*, 9, 3561-3574.

Rotunno, R., 1979: A study of tornado-like vortex dynamics. *J. Atmos. Sci.*, 36: 140-155.

Rotunno, R., and J. B. Klemp, 1985: On the rotation and propagation of simulated supercell thunderstorms. *J. Atmos. Sci.*, 42: 271-292.

Schaefer, J. T., and R. L. Livingston, 1998: The typical structure of tornado proximity soundings. *J. Geophys. Res.*, 93, 5351-5364.

Schlesinger, R. E., 1975: A three-dimensional numerical model of an isolated thunderstorm. Preliminary results. *J. Atmos. Sci.*, 32: 835-850.

Shewchuck, J., 2002: RAOB (the Rawinsonde Observation Program) for Windows. Version 5.1, Environmental Research Services. [Available from Environmental Research Services, 1134 Delaware Dr., Matamoras, Pennsylvania, 18336.

Sills, D., 1998: Lake and land breezes in southwestern Ontario: Observations, analyses and numerical modeling. PhD thesis, York University, Toronto.

Storm Prediction Center, 2008: *Fujita Tornado Damage Scale*. Retrieved July 26, 2008, from: http://www.spc.noaa.gov/faq/tornado/f-scale.html

Taylor, N. M., 1999: Climatology of sounding parameters identifying the potential for convective storm development over central Alberta. MSc thesis, University of Alberta, Edmonton.

Thomspson, R. L., R. Edwards, J. A. Hart, K. L. Elmore, and P. Markowski, 2003: Close proximity soundings within supercell environments obtained from the Rapid Update Cycle. *Wea. Forecasting*. 18: 1243-1261.

Turcotte, V., and D. Vigneux, 1987: Severe thunderstorms and hail forecasting using derived parameters from standard RAOBS data. Preprings, *Second*

Workship on Operational Meteorology, Halifax, Nova Scotia, Canada, Atmospheric Environment Service/Canadian Meteorological and Oceanographic Society, 142-153.

Verkaik, J., and Verkaik, A., 1997: *Under the Whirlwind:Everything You Need to Know About Tornadoes but DIdn't Know Who to Ask.* Whirlwind Books, 262 p.

Holton, J. R., 1979: *An Introduction to Dynamic Meteorology.* 2nd ed. Academic Press, New York, New York, 300 p.

Wakimoto, R. M., and J. W. Wilson, 1989: Non-supercell tornadoes. *Mon. Wea. Rev.*, 117: 1113-1140.

Weisman, M. L., and J. B. Klemp, 1982: The dependence of numerically simulated convective storms on vertical wind shear and buoyancy. *Mon. Wea. Rev.*, 110: 504-520.

Weisman, M. L., and J. B. Klemp, 1986: Characteristics of isolated storms. *Mesoscale Meteorology and Forecasting*, P. S. Ray, Ed., Amer. Meteor. Soc., 331-357.

Wilson, J., A. Crock, C. K. Mueller, J. Sun, M. Dixon, 1998: Nowcasting thunderstorms: A status report. *Bulletin of the American Meteorological Society*, 79(10): 2079-2100.

Wittmeyer, I. L., and T. H. Vonder Haar, 1994: Analysis of the global ISCCP TOVS water vapor climatology. *J. Climate*, 7, 325-333.

Wright, J. M. Jr., Federal meteorological handbook No. 3, 1997: *Rawinsonde and pibal observations*. Retrieved March 13, 2008, from: http://www.ofcm.gov/fmh3/text/default.htm

Zeigler, C. L., E. N. Rasmussen, T. R. Shepherd, A. I. Watson, and J. M. Straka, 2001: The evolution of low-level rotation in the 29 May 1994 Newcastle-Graham, Texas storm complex during VORTEX. *Mon. Wea. Rev.*, 129, 1339-1368.

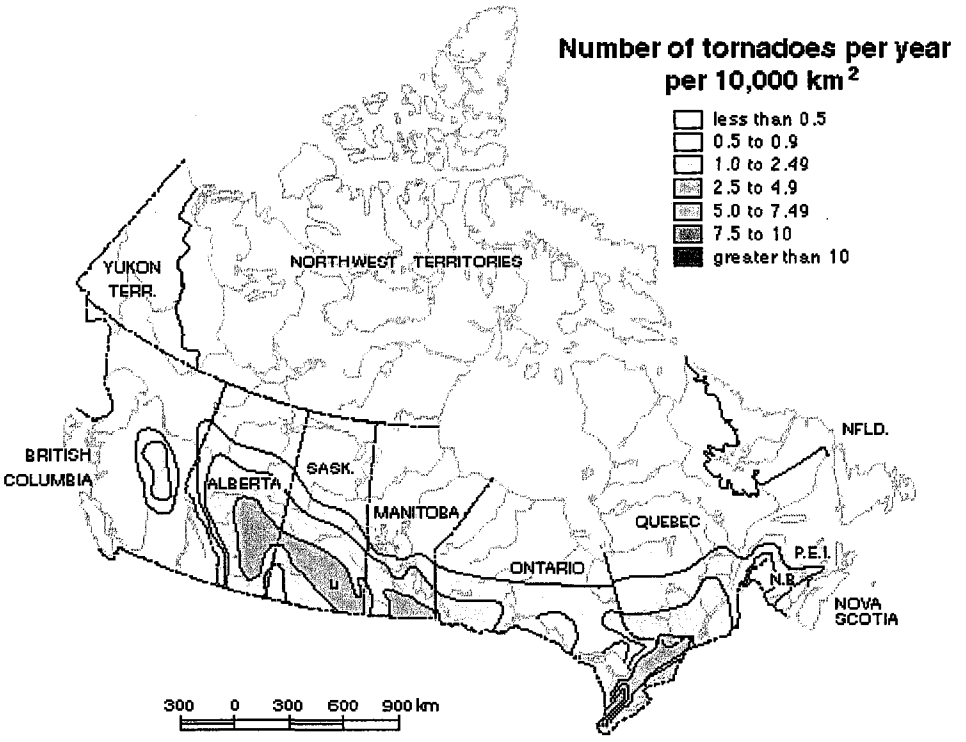

Figure 1.1: Average number of tornadoes per 10 000 km^2 annually across Canada. Adapted from Newark, 1984.

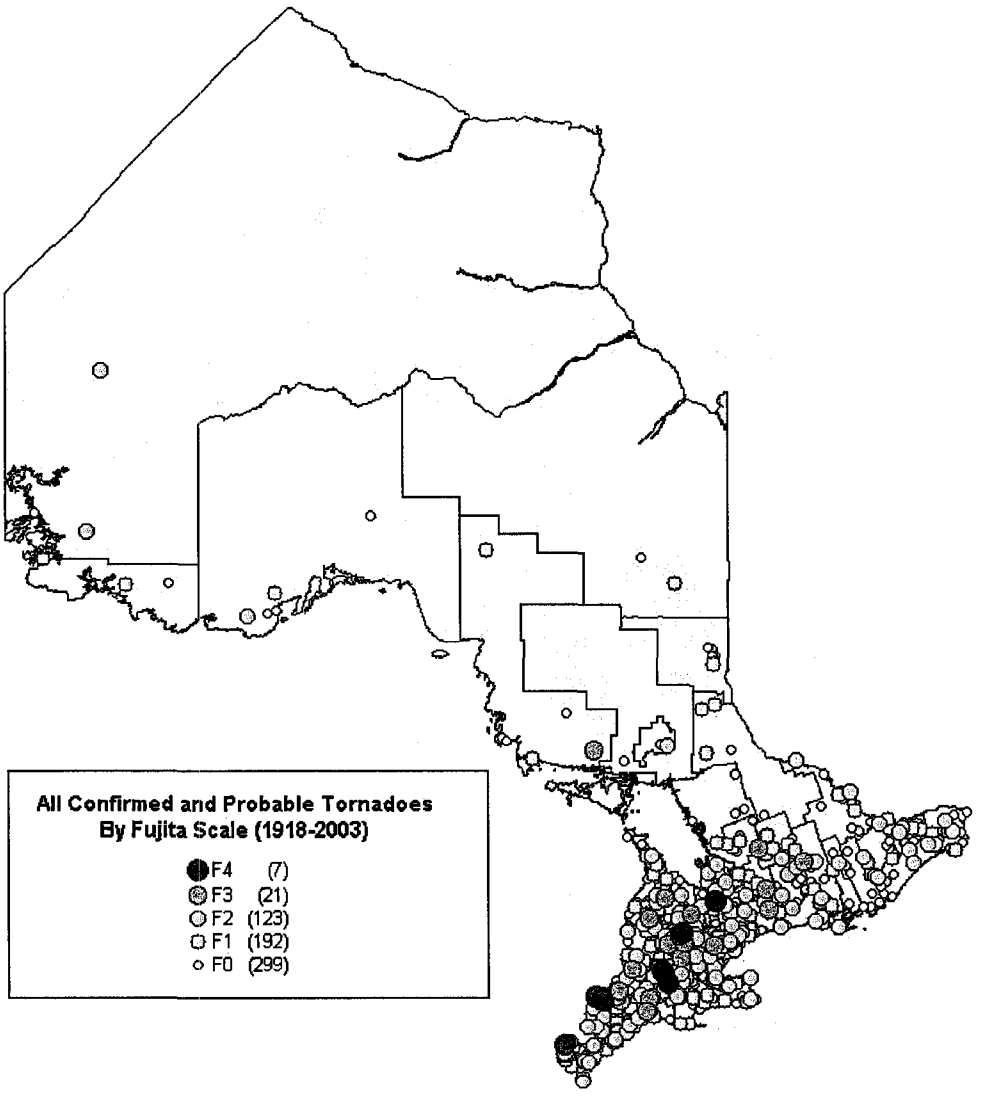

Figure 1.2: All confirmed and probable tornadoes (1918-2003) for Ontario and southern Ontario categorized by Fujita Scale and indicated by dot color. (Adapted from Auld et al., 2004). **Source:** Meteorological Service of Canada-Ontario Region, 2003a.

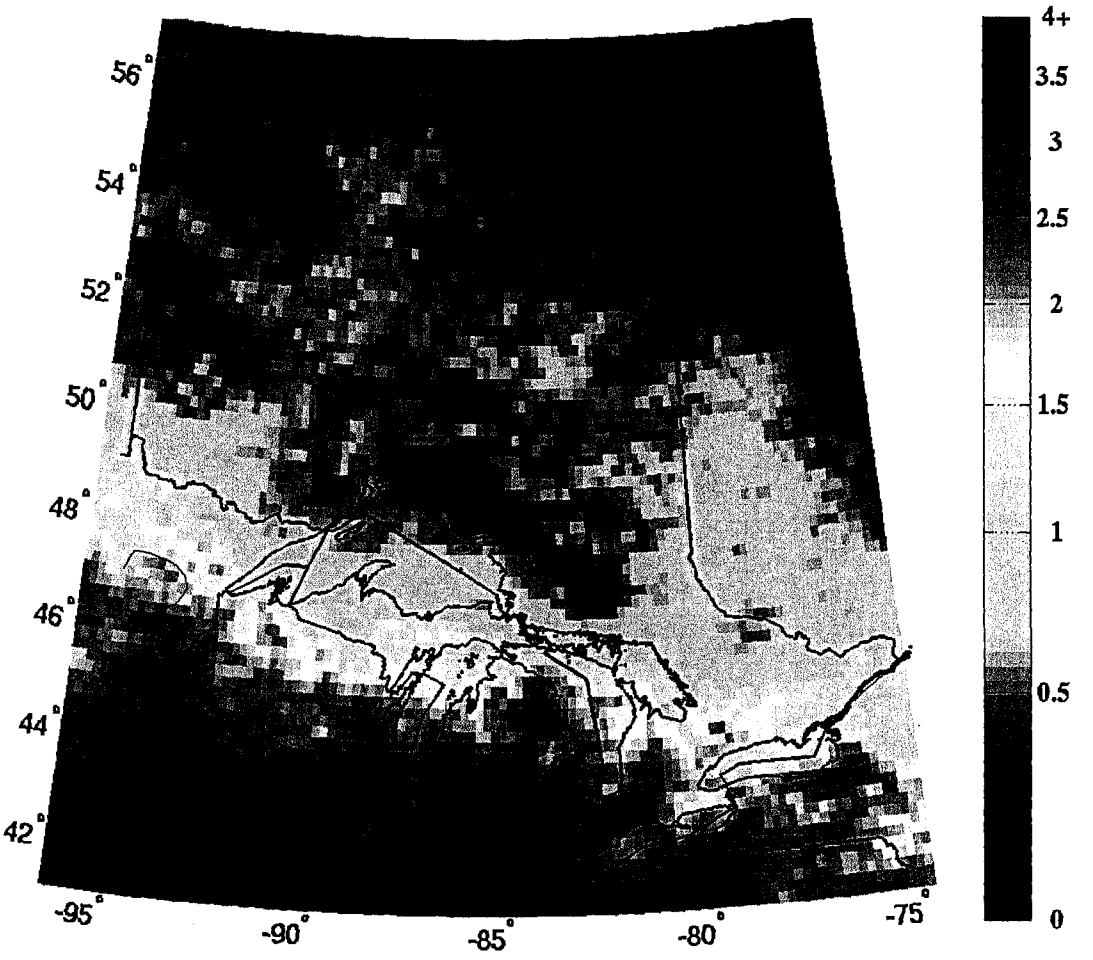

Figure 1.3a: Average annual flash density (number of flashes per km^2 per year) from cloud-to-ground and cloud-to-cloud lightning combined from 1998-2006. (Adapted from Auld et al., 2004). **Source:** Meteorological Service of Canada-Ontario Region, 2003c.

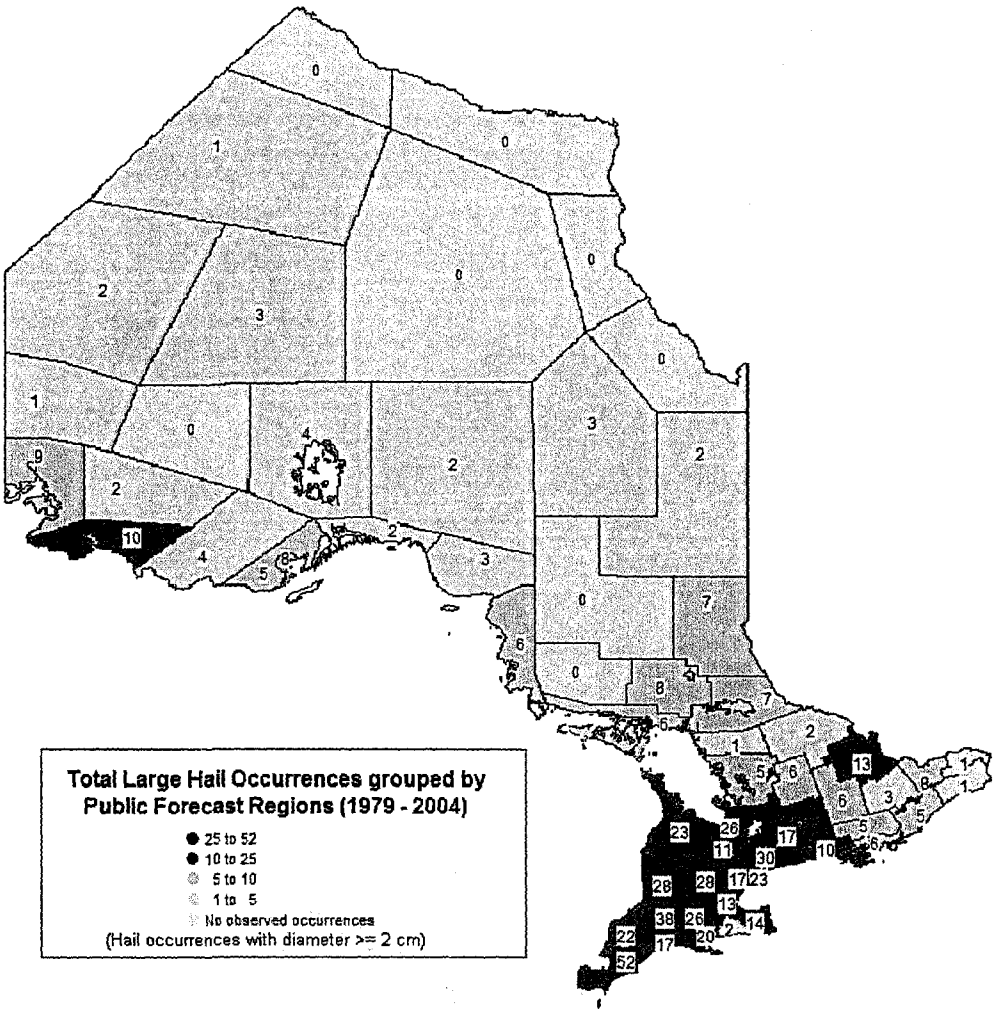

Figure 1.3b: Total potentially damaging hail events by Environment Canada Public Forecast Region from 1979 to 2004. A significant damaging hail event was considered to have occurred when hail of 2 cm or greater was observed. (Adapted from (Adapted from Auld et al., 2004). **Source:** Meteorological Service of Canada-Ontario Region, 2003b.

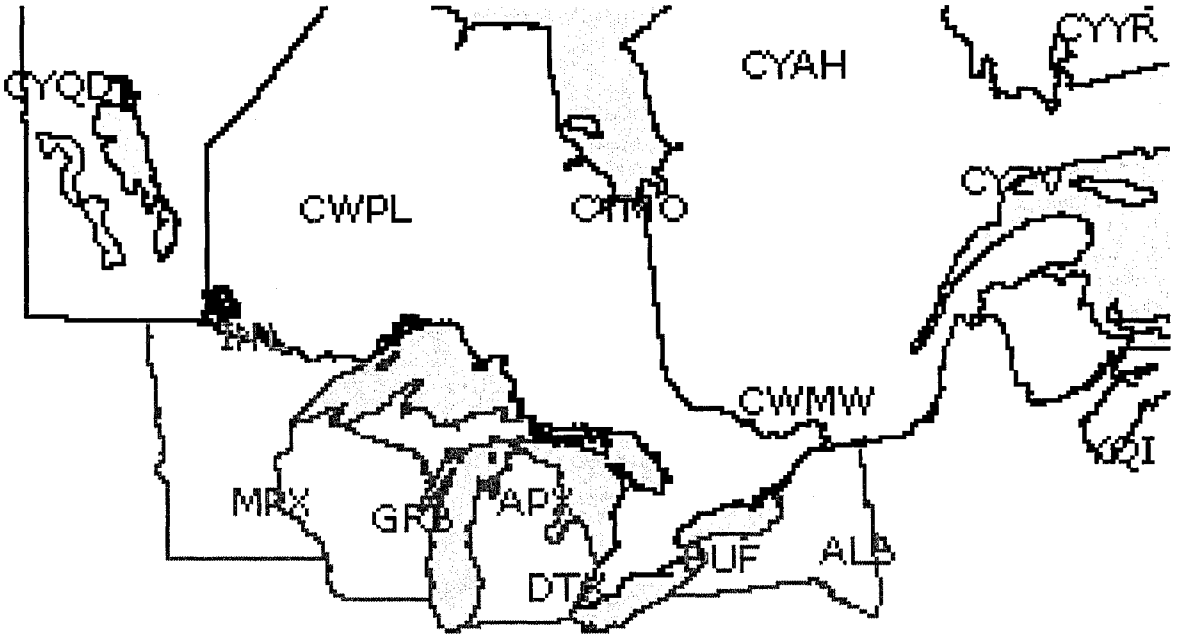

Figure 2.1: Map of central Canada and the Great Lakes region of the United States showing the upper air reporting stations: The Pas (CYQD), Pickle Lake (CWPL), Moosonee (CYMO), Maniwaki (CWMW), La Grande Iv (CYAH), Sept-Iles (CYZV), Goose Bay (CYYR), Yarmouth (YQI), International Falls (INL), Canhassen (MPX), Green Bay (GRB), Gaylord (APX), White Lake (DTX), Buffalo International (BUF), Albany (ALB). Adapted from The National Center for Atmospheric Research at: http://www.rap.ucar.edu/weather/upper/.

Figure 2.2: Outline of Ontario showing the location of the upper air station (BUF) at Buffalo, New York and the cities of Windsor, London, Toronto and Ottawa. The circle marks a 200 km radius from BUF.

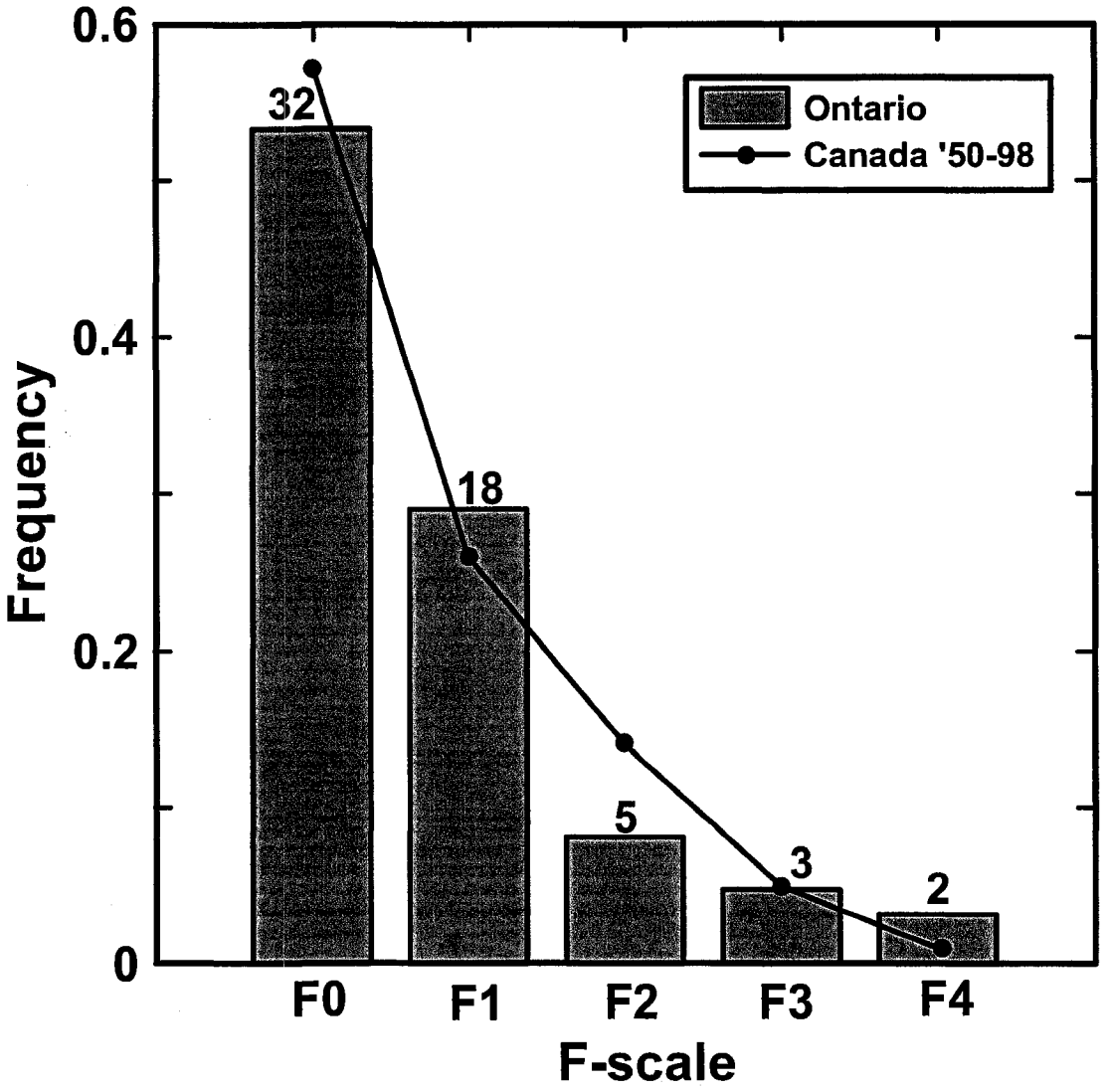

Figure 2.3: The frequency of tornadoes categorized by Fujita Scale (F-scale). The bars indicate the frequency of tornado cases for this study in southern Ontario between 1961 and 1996. The total number of tornado soundings is 60. The value above each bar shows the number of cases per F-scale group. The line and dots indicate the frequency of tornado events in all of Canada from 1950 to 1998.

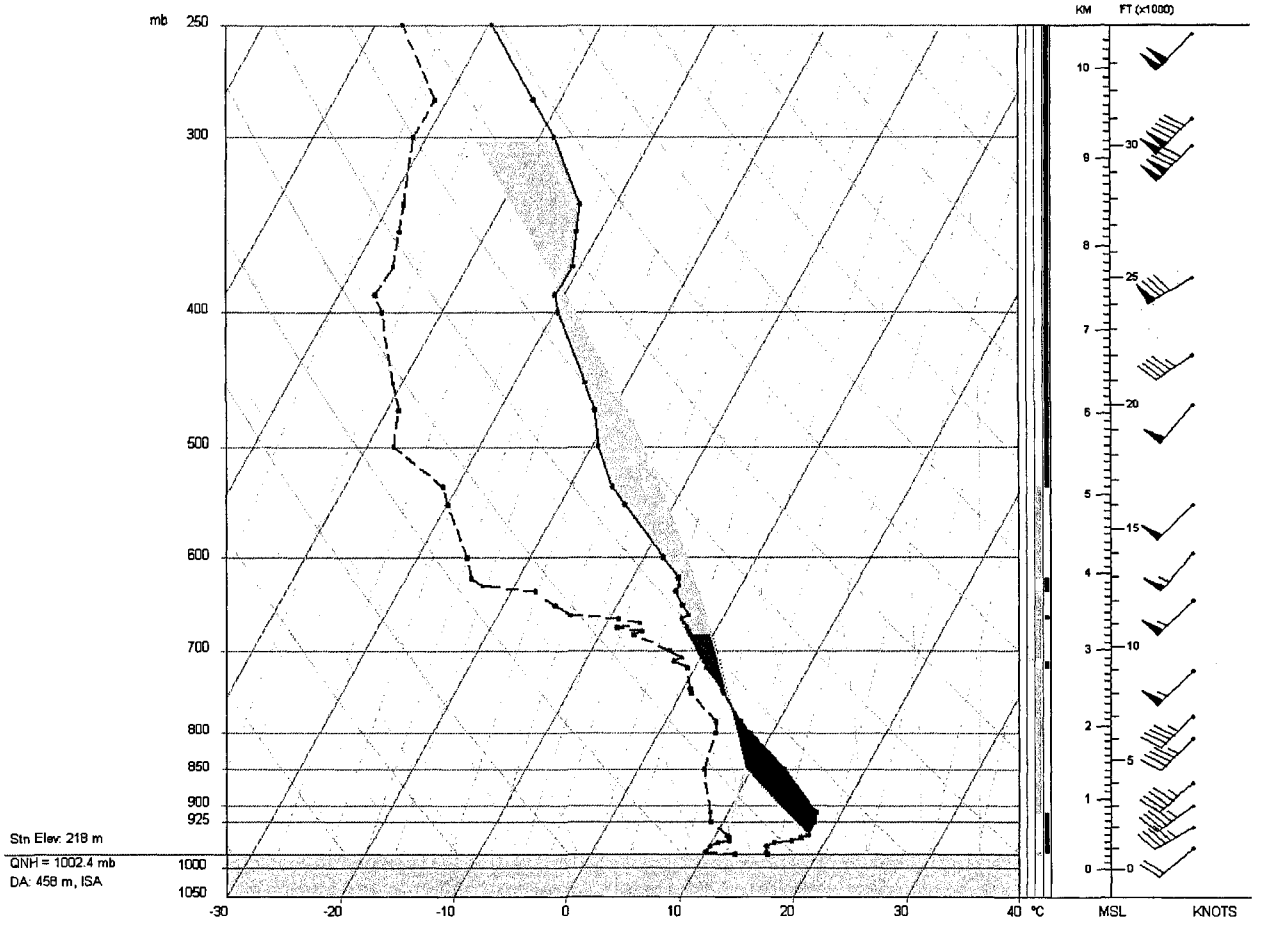

Figure 2.4: A typical sounding for the Buffalo, New York (BUF) upper-air site taken at 0000 UTC on April 21, 1996. The solid red curve displays the temperature profile in °C, and the dotted red curve displays the dewpoint temperature in °C. The cyan curve on the far right is the best possible level parcel ascent curve, and the red shaded area represents the CAPE. Wind barbs are plotted on the far right in knots where half barbs denote 2.5 kts and full barbs denote 5 kts.

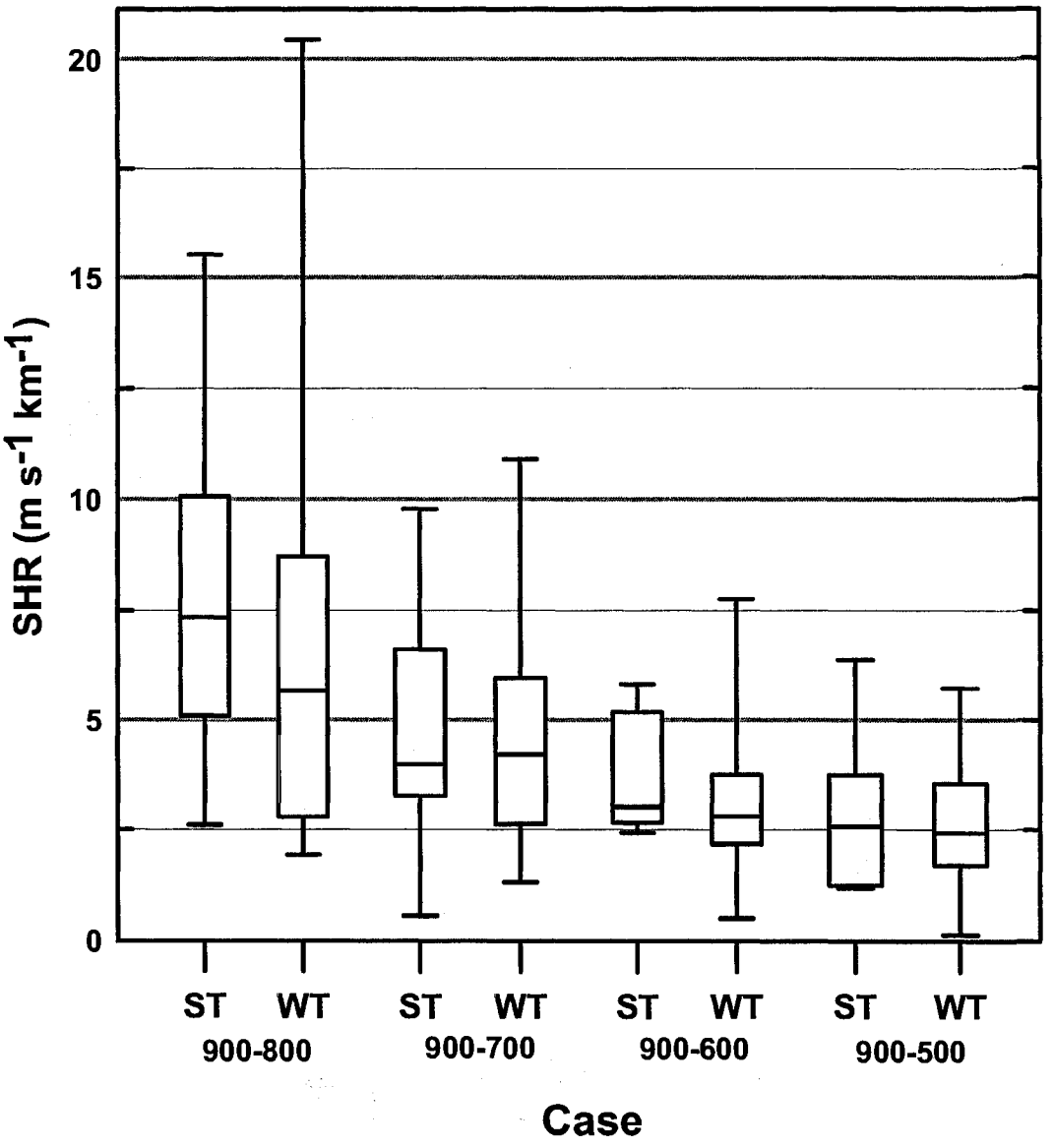

Figure 3.1: Bulk shear (SHR) values displayed in a box and whiskers plot. Values are shown for strong and weak tornadoes (ST, WT) for the layers 900-800 mb, 900-700 mb, 900-600 mb and 900-500 mb. The grey boxes denote the 25th and 75th percentiles with a heavy black line at the median value. The vertical lines (whiskers) indicate the maximum and minimum values.

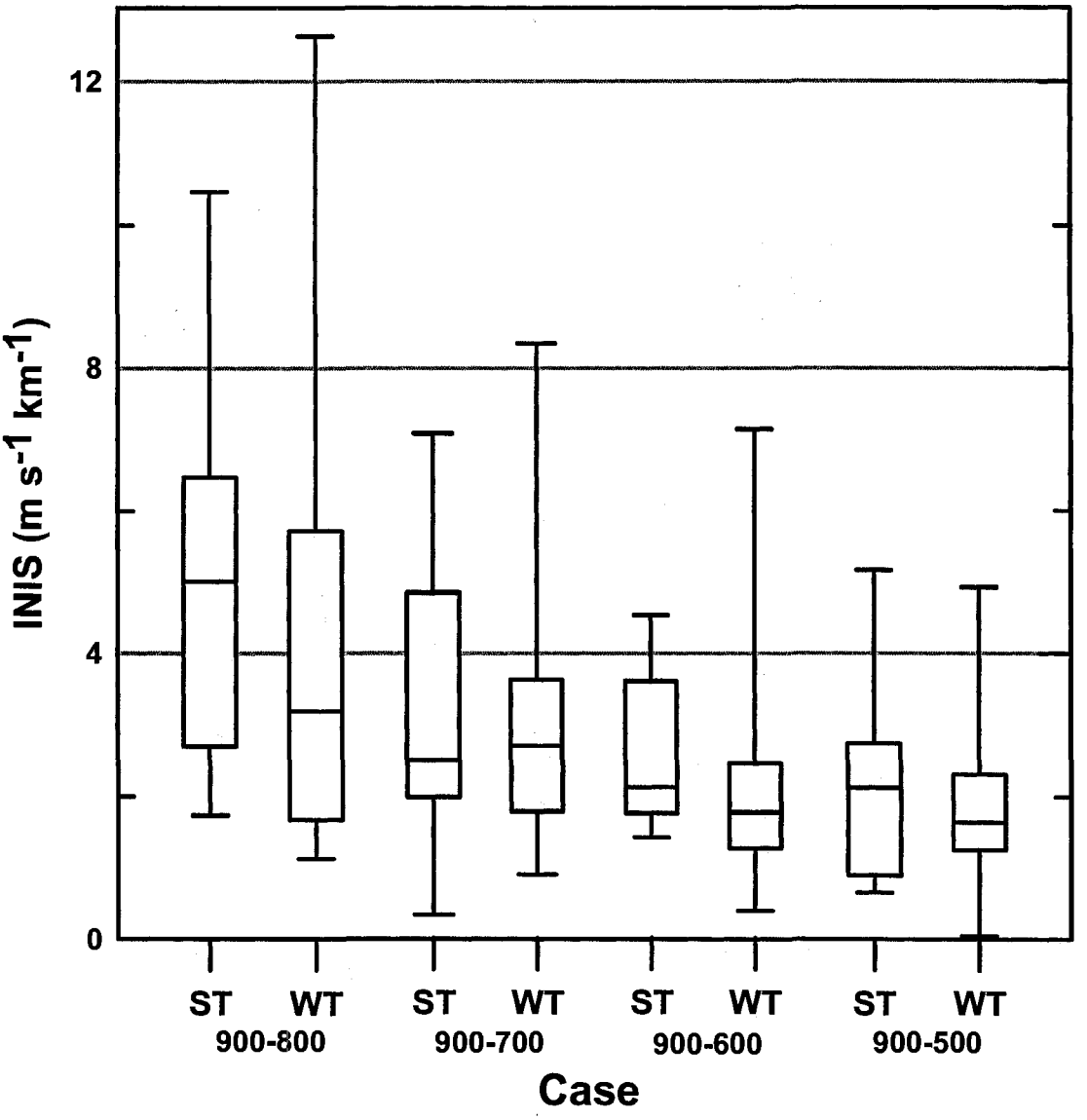

Figure 3.2: INIS values displayed in a box and whiskers plot for strong and weak tornadoes (ST, WT) for pressure layers 900-800 mb, 900-700 mb, 900-600 mb and 900-500 mb.

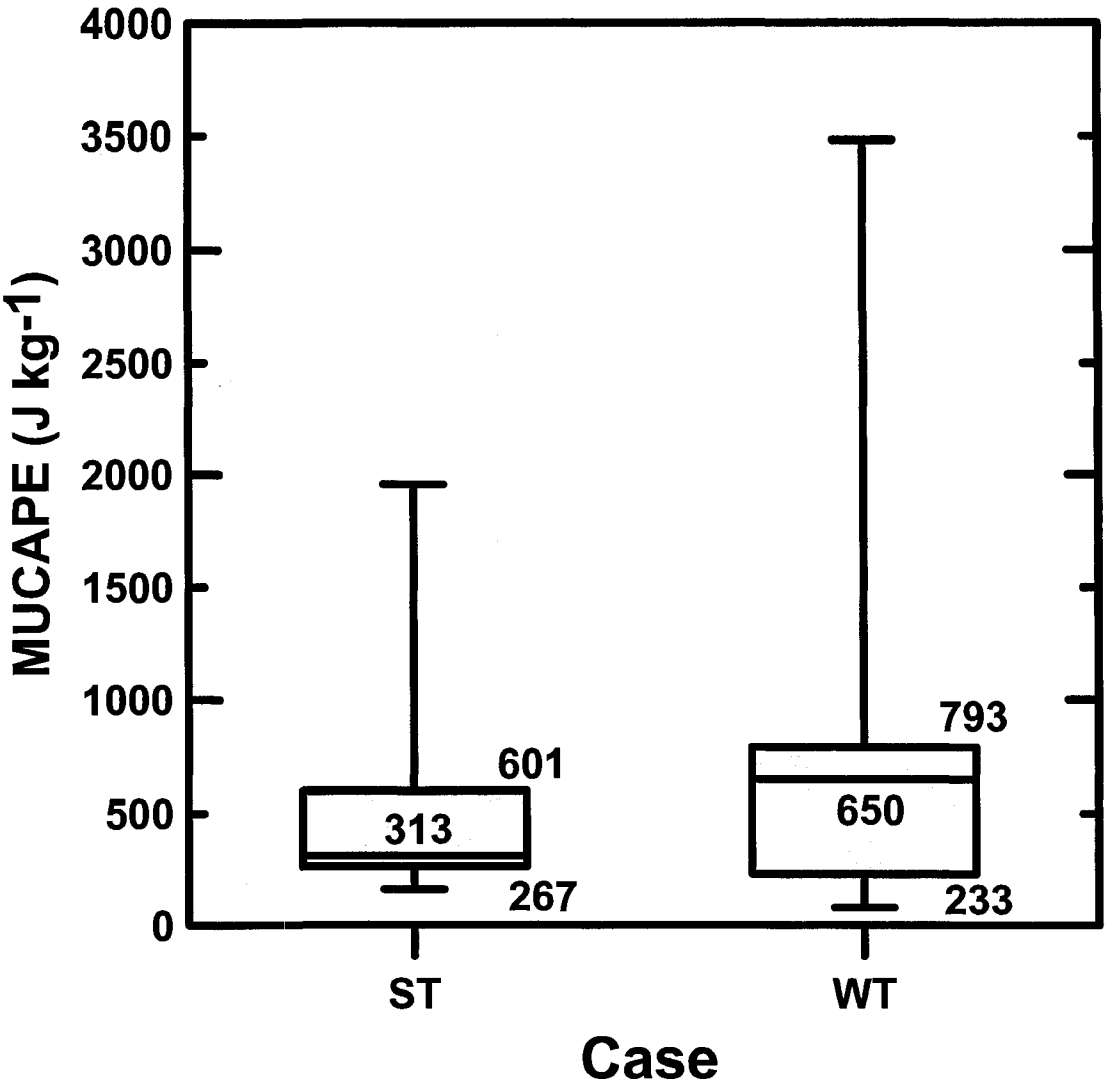

Figure 3.3: Box and whiskers plot of most-unstable convective available potential energy (MUCAPE) values for strong and weak tornadoes (ST, WT).

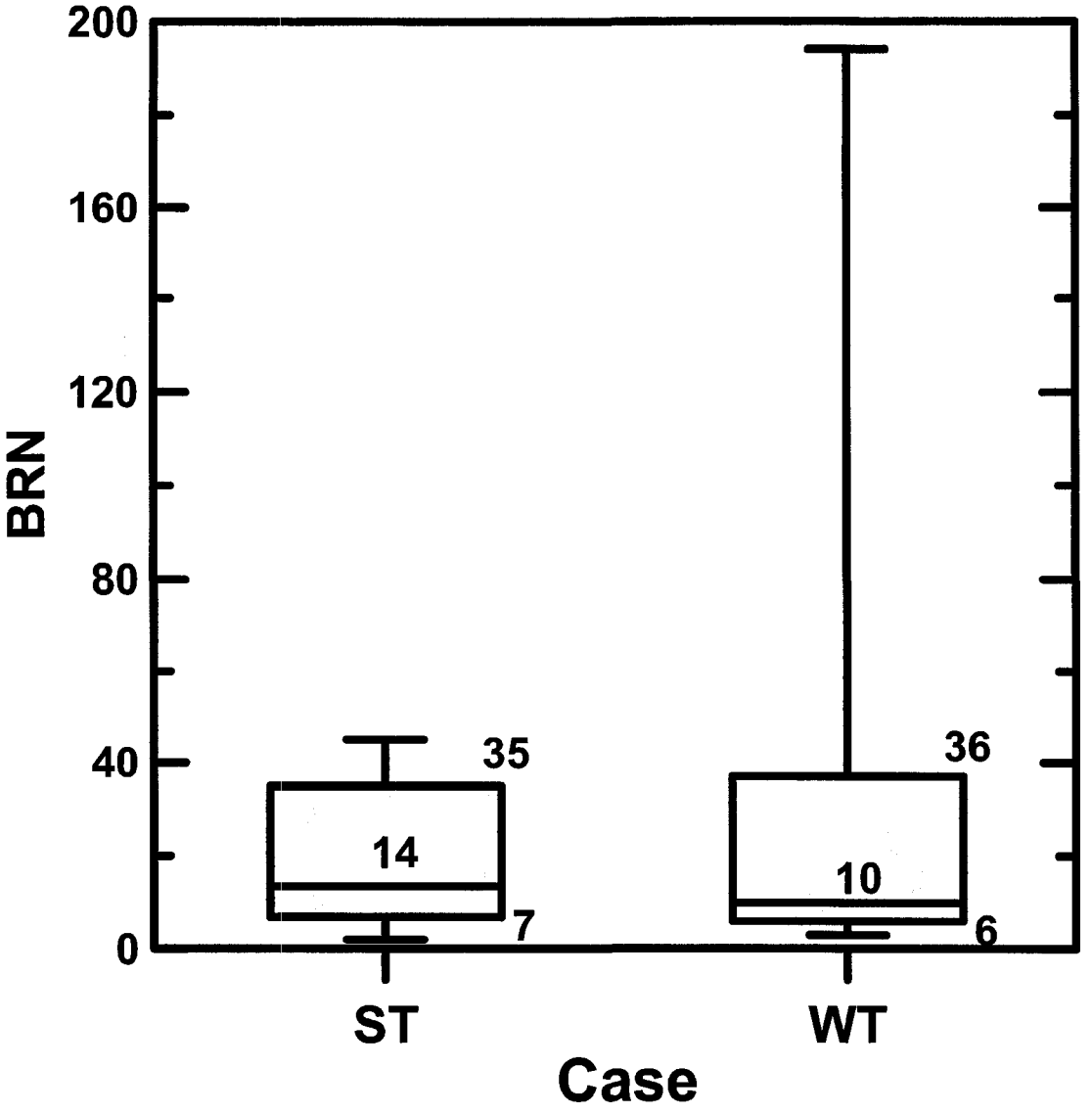

Figure 3.4: Box and whiskers plot of bulk Richardson number (BRN) values for strong and weak tornadoes (ST, WT).

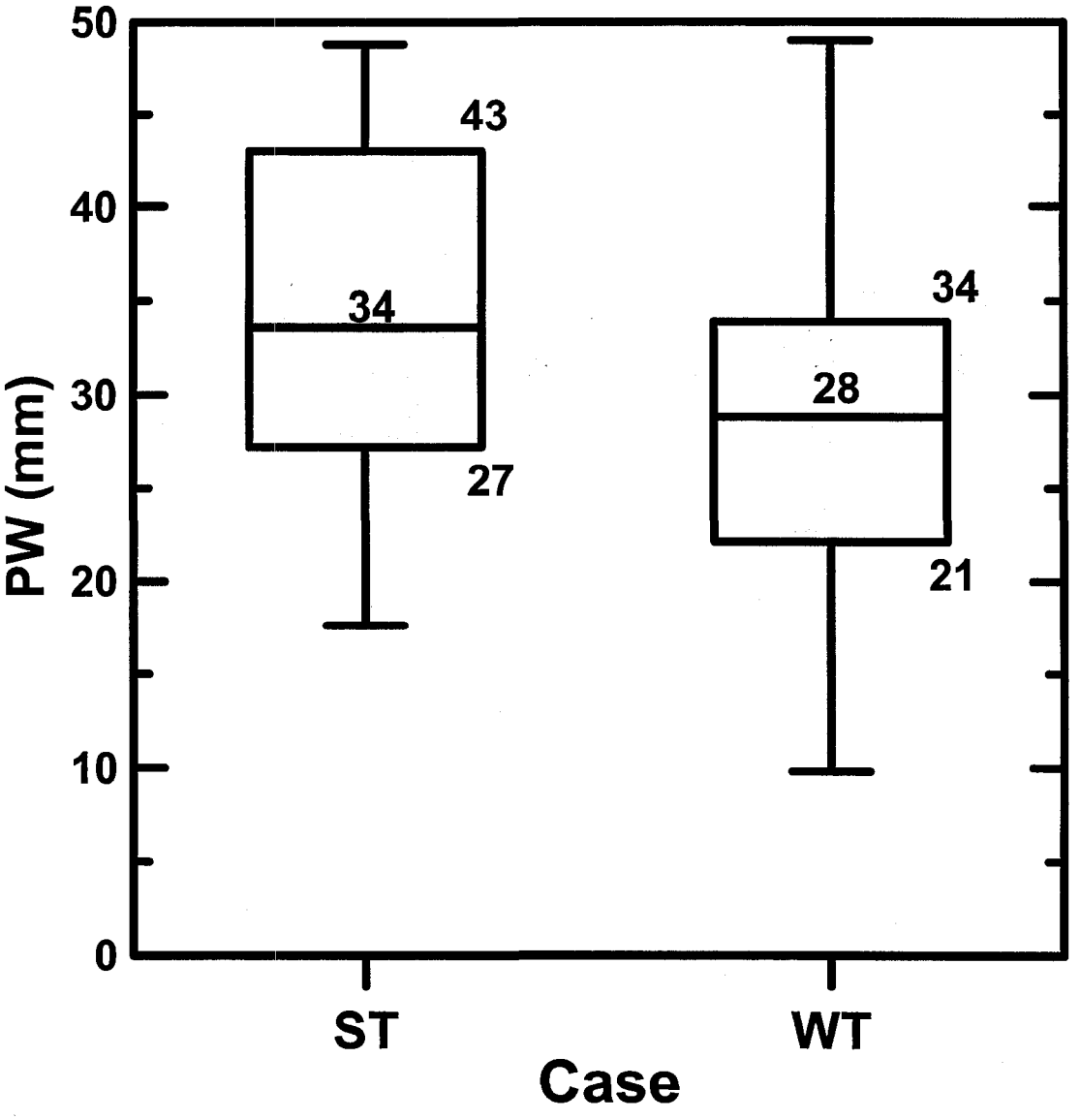

Figure 3.5: Box and whiskers plot of precipitable water (PW) values for strong and weak tornadoes (ST, WT).

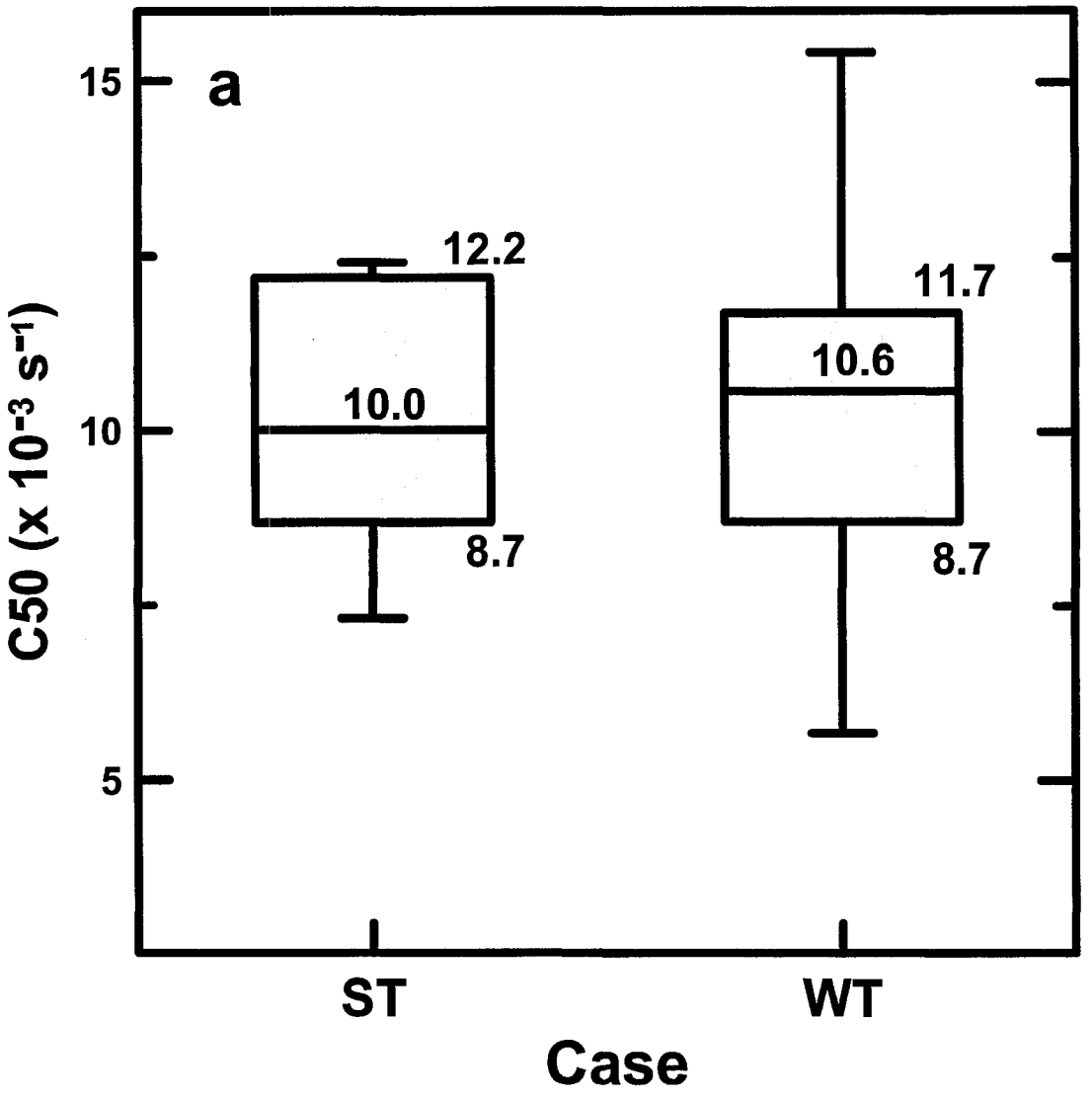

Figure 3.6a: Box and whiskers plot of storm convergence values for strong and weak tornadoes (ST, WT) in the layer from the level of free convection (LFC) to 50 mb above the LFC.

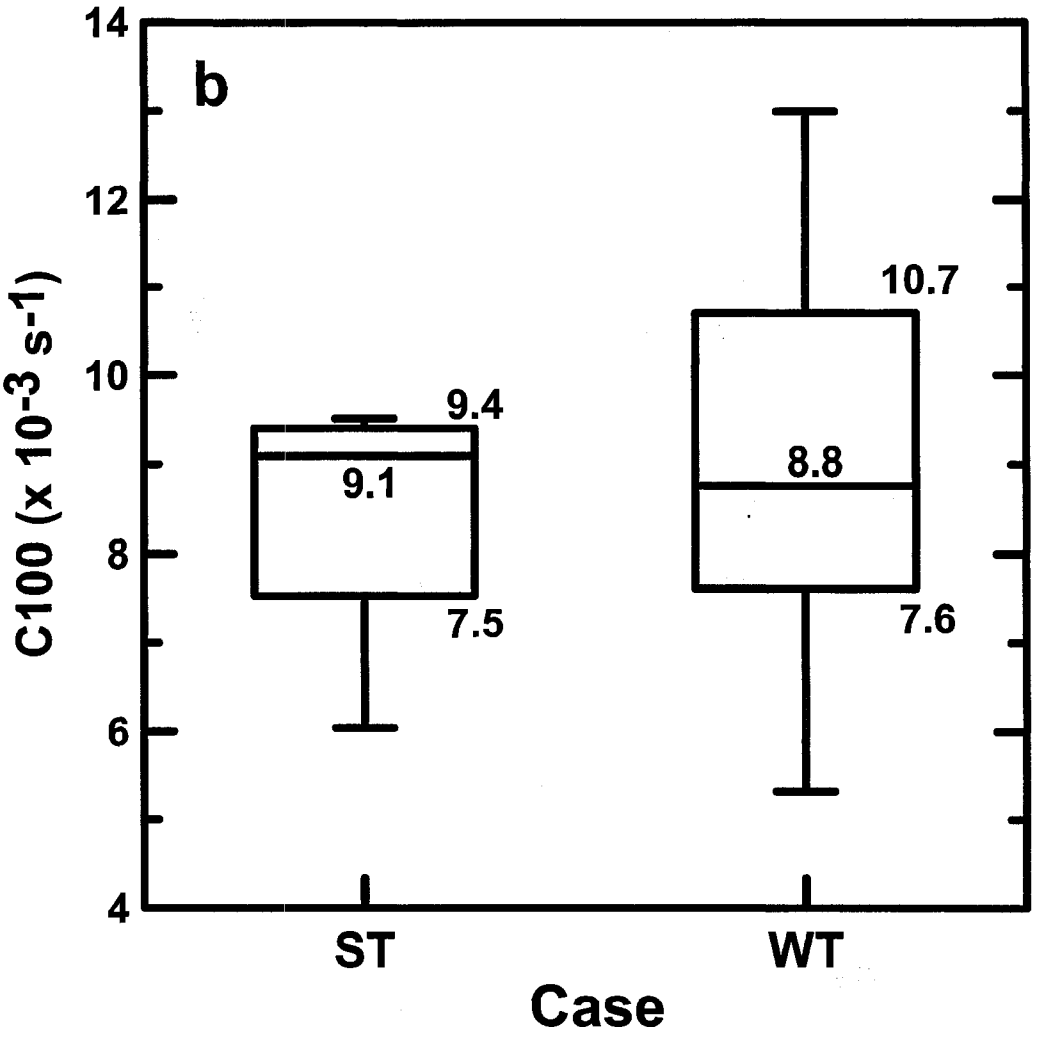

Figure 3.6b: Box and whiskers plot of storm convergence values for strong and weak tornadoes (ST, WT) in the layer from the LFC to 100 mb above the LFC.

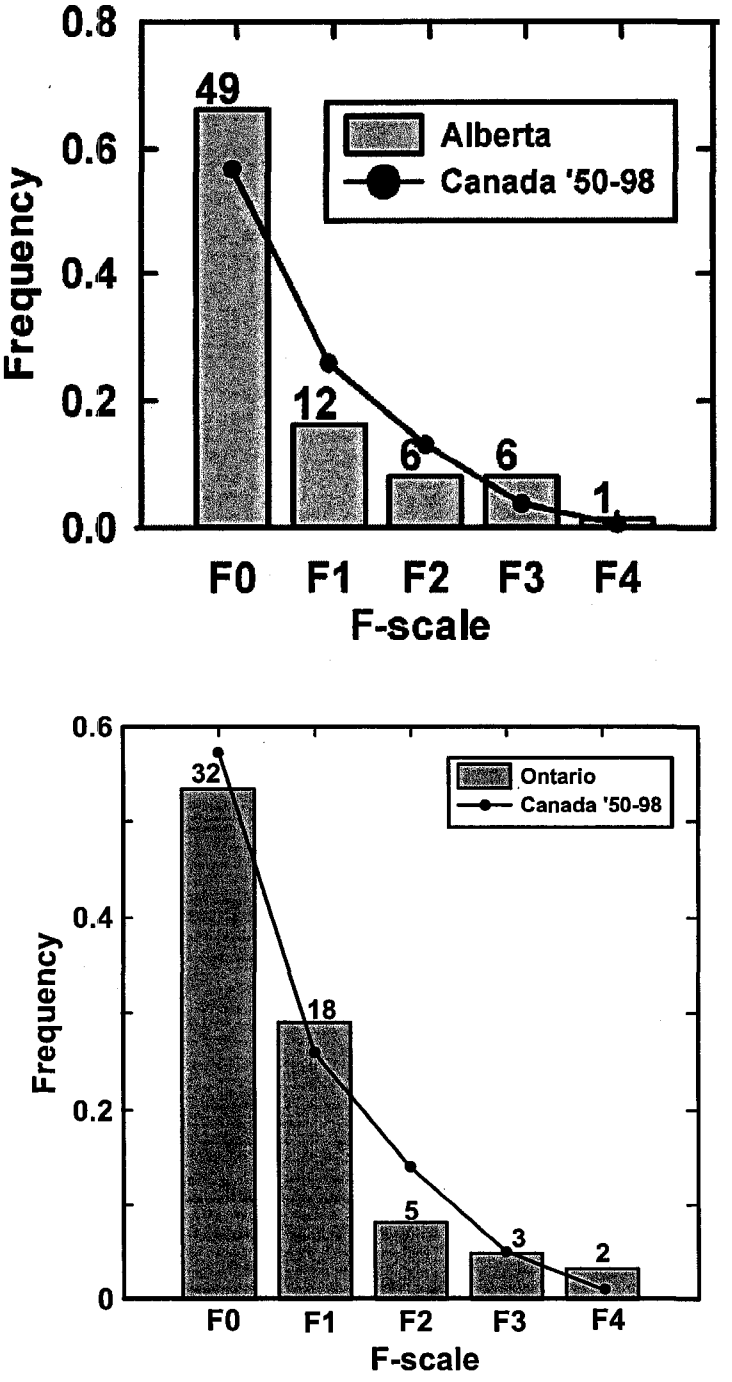

Figure 4.1: The frequency of tornadoes categorized by Fujita Scale (F-scale) for Alberta (top) and southern Ontario (bottom). The bars indicate the frequency of tornado cases between 1967-2000 (Alberta) and 1961-1996 (Ontario). The total number of tornado soundings is 74 for Alberta and 60 for Ontario. The value above each bar shows the number of cases per F-scale group. The line and dots on both plots indicate the frequency of tornado events in all of Canada from 1950 to 1998.

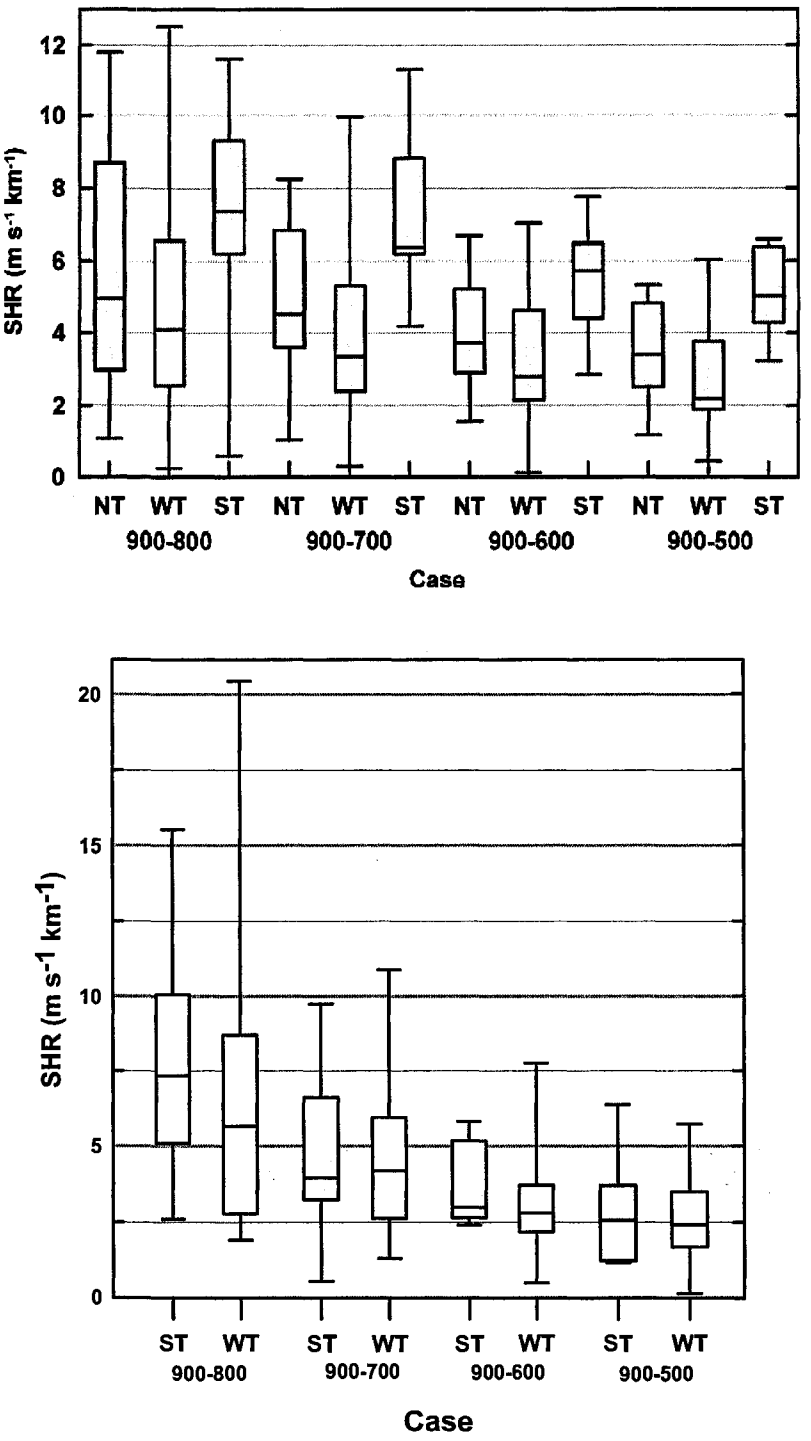

Figure 4.2: Bulk shear (SHR) values displayed in a box and whiskers plot for the Alberta dataset (top) and the southern Ontario dataset (bottom). NT denotes non-tornadic storms, WT denotes weak tornadoes and ST denotes strong tornadoes. Values are shown for the layers 900-800 mb, 900-700 mb, 900-600 mb and 900-500 mb.

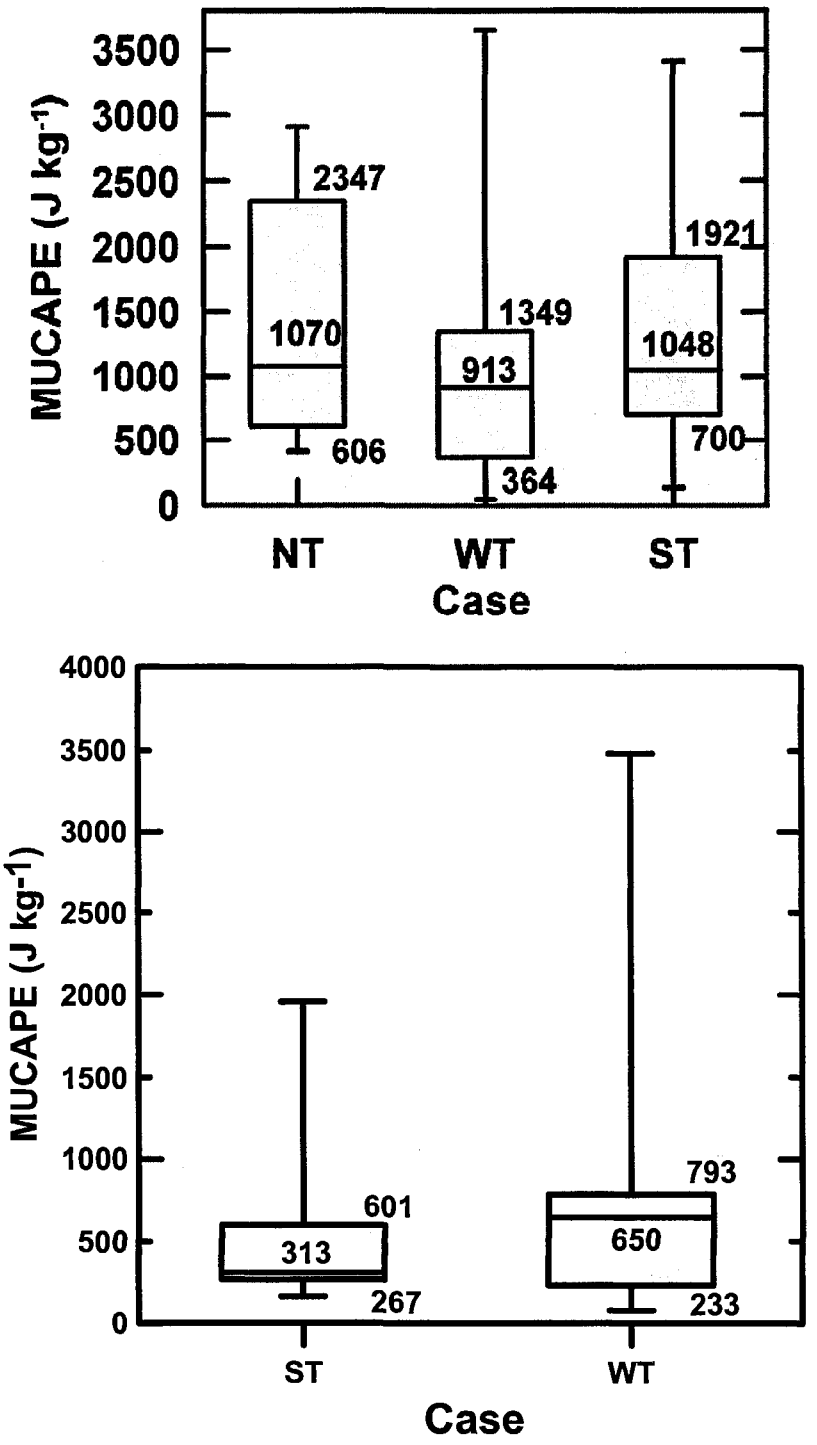

Figure 4.3: Most-unstable CAPE (MUCAPE) values displayed in a box and whiskers plot for the Alberta dataset (top) and the southern Ontario dataset (bottom). NT denotes non-tornadic storms, WT denotes weak tornadoes and ST denotes strong tornadoes.

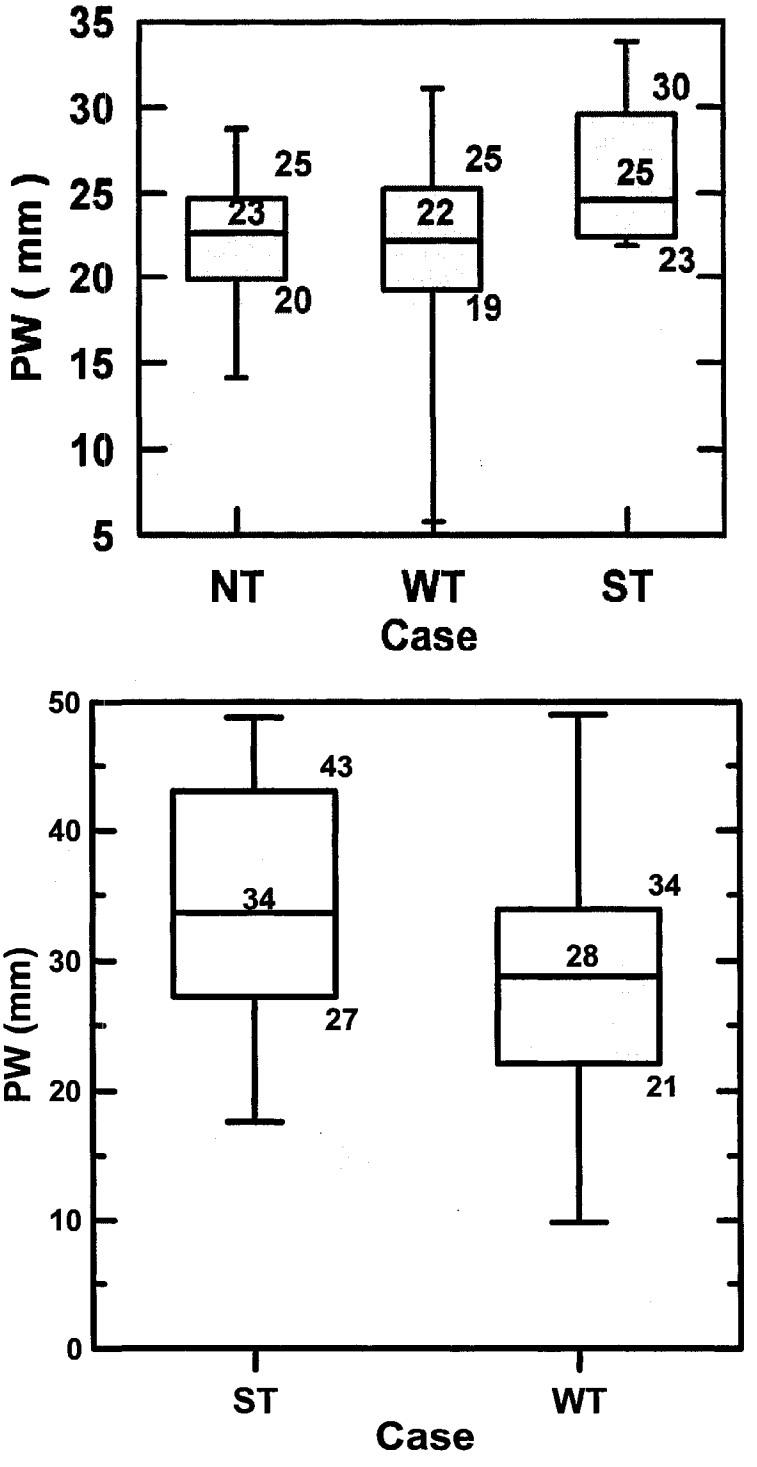

Figure 4.4: Precipitable water (PW) values displayed in a box and whiskers plot for the Alberta dataset (top) and the southern Ontario dataset (bottom). NT denotes non-tornadic storms, WT denotes weak tornadoes and ST denotes strong tornadoes.

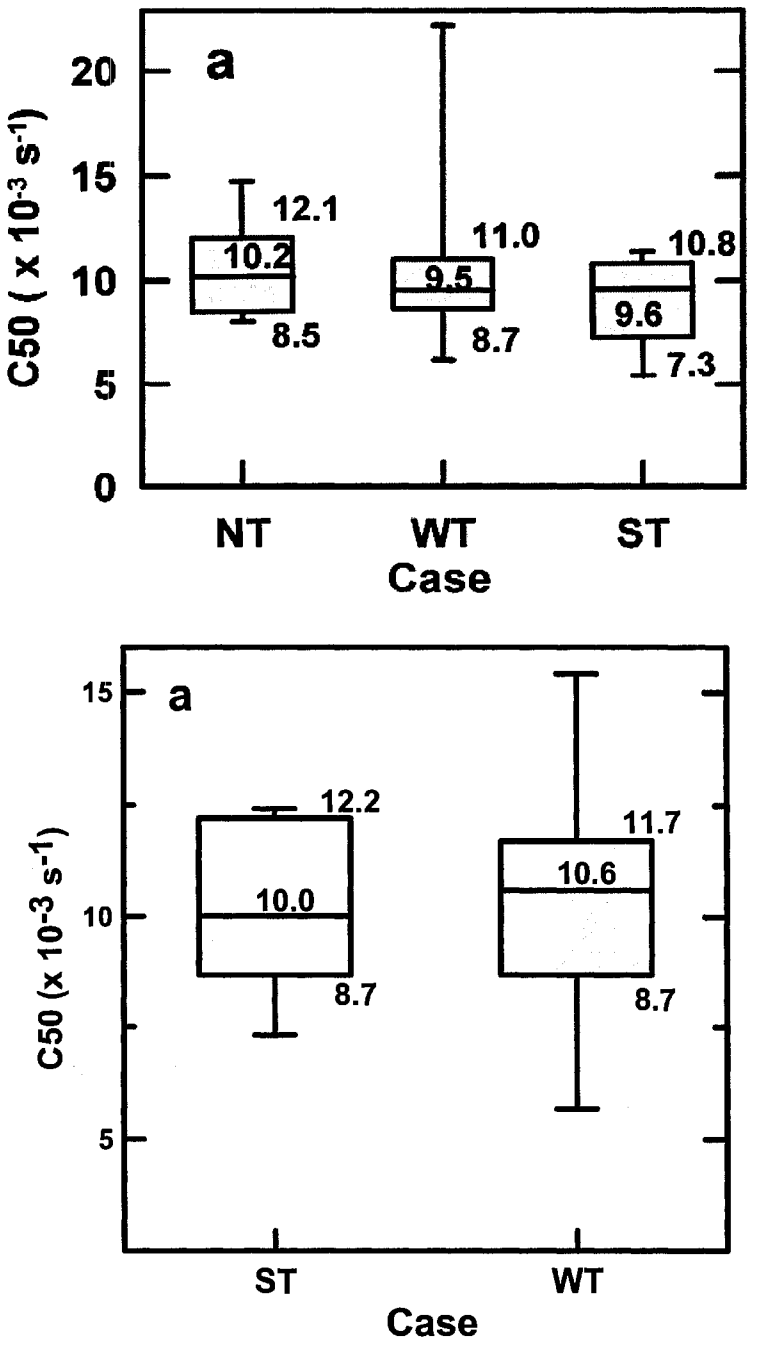

Figure 4.5a: Box and whiskers plot of storm convergence values in the layer from the LFC to 50 mb above the LFC for the Alberta dataset (top) and the southern Ontario dataset (bottom). NT denotes non-tornadic storms, WT denotes weak tornadoes and ST denotes strong tornadoes.

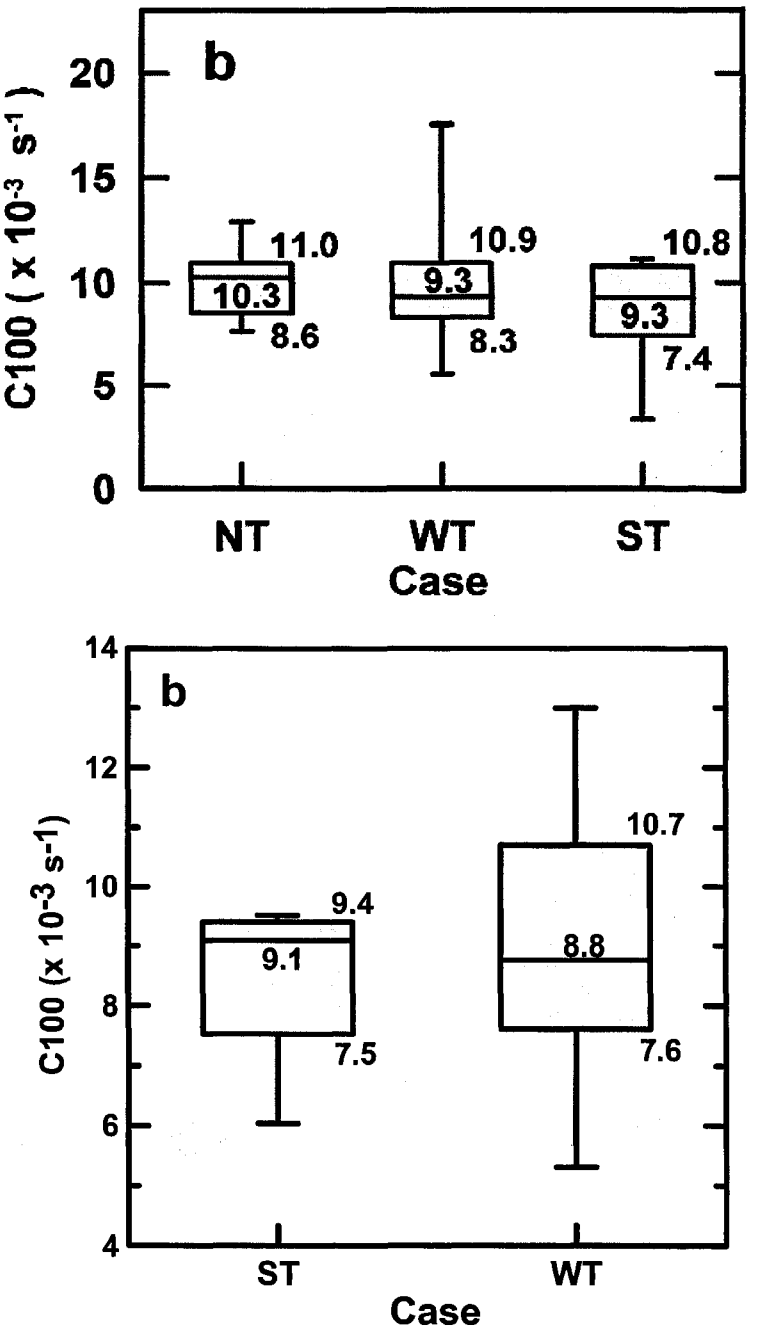

Figure 4.5b: Box and whiskers plot of storm convergence values in the layer from the LFC to 100 mb above the LFC for the Alberta dataset (top) and the southern Ontario dataset (bottom). NT denotes non-tornadic storms, WT denotes weak tornadoes and ST denotes strong tornadoes.

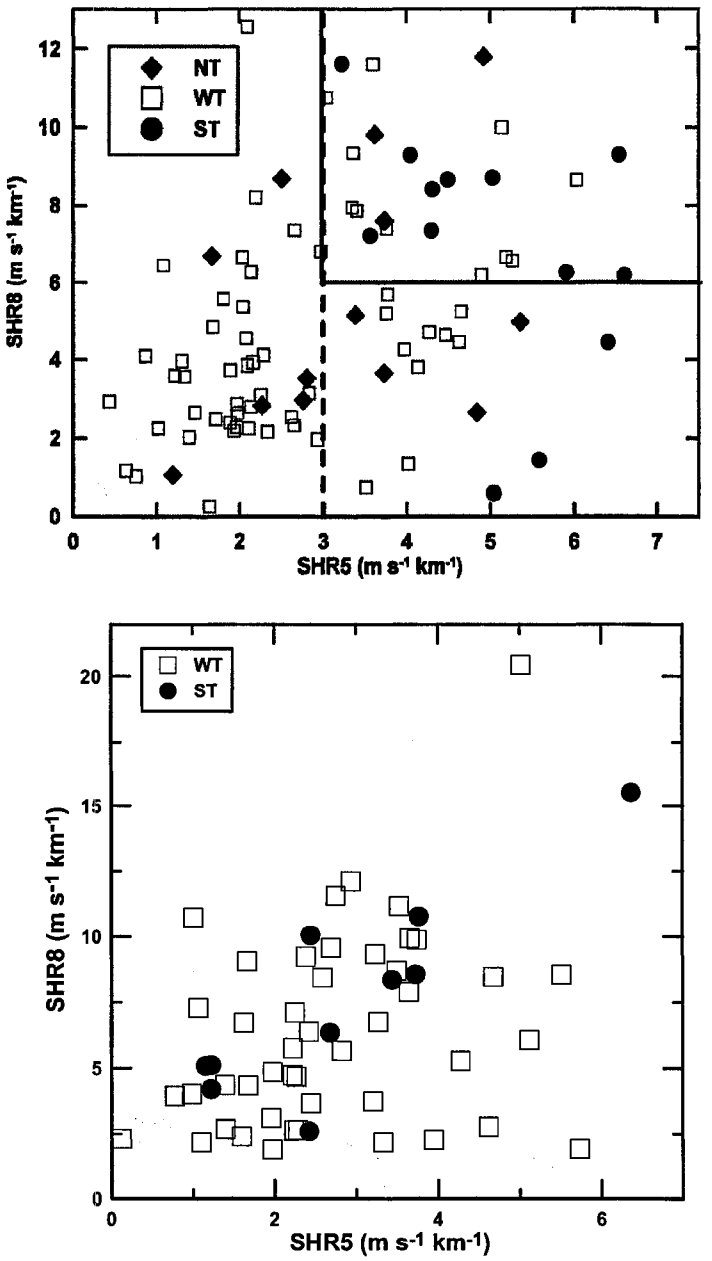

Figure 4.6: Scatter plots of SHR8 versus SHR5 values for the Alberta dataset (top) and the Ontario dataset (bottom). Non-tornadic storms (NT) are denoted by solid diamonds, weak tornadoes (WT) are denoted by open squares and strong tornadoes (ST) are denoted by solid circles. In the top figure, the solid line indicates the 77% threshold for ST events, and the dotted line indicates the 100% threshold.

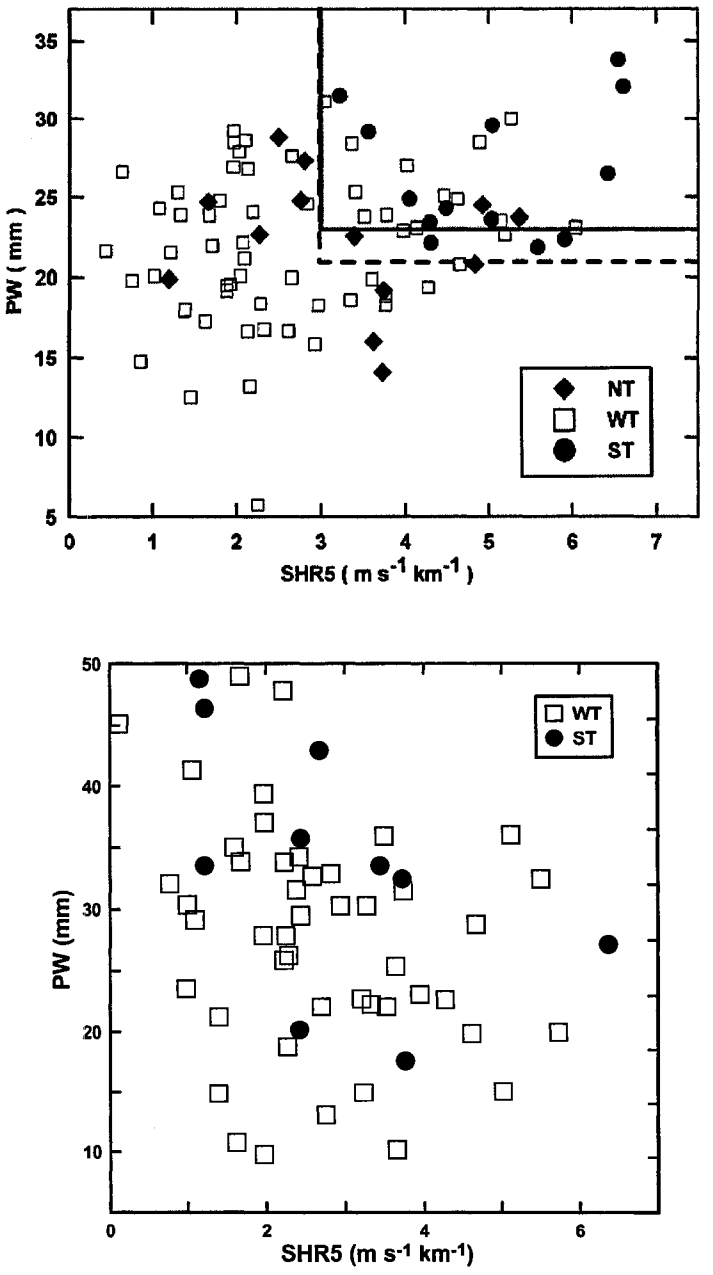

Figure 4.7: Scatter plots of PW versus SHR5 values for the Alberta dataset (top) and the Ontario dataset (bottom). Non-tornadic storms (NT) are denoted by solid diamonds, weak tornadoes (WT) are denoted by open squares and strong tornadoes (ST) are denoted by solid circles. In the top figure, the solid line indicates the 77% threshold for ST events, and the dotted line indicates the 100% threshold.

Appendix A

Radiosonde Instrument Package

The radiosonde instrument package is carried aloft from the earth's surface by a helium or hydrogen-filled balloon made of natural or synthetic rubber (neoprene) which typically reaches altitudes of about 30 km before it bursts (Hopkins 1996). At launch the balloon is approximately 2 m in diameter and expands to about 8 m before it bursts (Figure A). The balloon is capable of providing sufficient lift to carry a radiosonde payload of several pounds. The attached parachute returns the instrument package safely to the ground, and if they are recovered, they can be refurbished for further launches (Hopkins 1996).

As the balloon ascends, observed air temperature and humidity are measured and simultaneously transmitted via radio to a ground station (Wright 1997). Wind direction and wind speed is determined at various altitudes during the ascent by tracking the balloon's movement using a radiosonde package with a radio direction finder called a *rawinsonde*. The complete rawinsonde instrument package thus provides observations of the atmosphere describing the vertical profile of air temperature, humidity, wind speed and wind direction as a function of pressure (or height) from the surface to an altitude of approximately 30 km (at a pressure of approximately 10 mb) where the balloon bursts about 90 minutes after launch. The entire instrument package consists of a balloon-borne radiosonde, a radio tracking/receiving unit and a recorder for data processing.

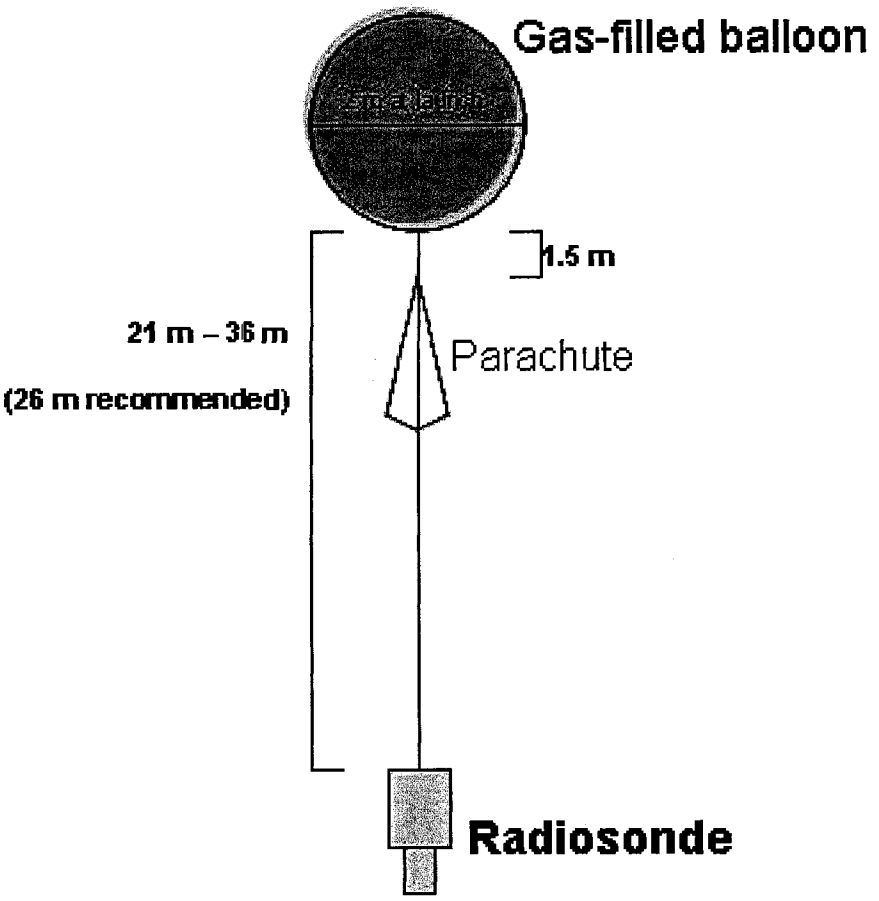

Figure A: Schematic of a radiosonde with gas-filled balloon, parachute and instrument package. Adapted from Wright ,1997.

The radiosonde instrument package is contained in a sturdy, lightweight box and consists of sensors, either within or attached to the package, which measure pressure, temperature and humidity from launch to balloon burst.

The pressure measured by a radiosonde is usually accomplished using an aneroid barometer; a small, evacuated metal canister which expands in response to the reduction of atmospheric pressure as the radiosonde ascends. The amount of expansion is proportional to the absolute pressure and is indicated by

the movement of a mechanical arm, a capacitance, or a voltage. The temperature compensated instrument is capable of measuring pressures from 1040 mb to 10 mb at temperatures ranging from -90 °C to 50 °C (Wright 1997). Another instrument used for measuring atmospheric pressure is a hypsometer, which uses the known boiling point of a liquid to determine the ambient pressure via the Clausius-Clapeyron equation. Pressure levels may also be computed from the hypsometric equation using temperature and humidity measurements from the radiosonde, along with the height determined by radar. This method eliminates the need for a pressure sensor altogether (Dupilka 2006).

The temperature is usually measured by a resistance thermistor, a white, ceramic-covered metallic rod whose electrical resistance or capacitance changes with air temperature. The thermistor is located on an outrigger which extends outside of the radiosonde instrument package in order to increase its contact with air, and it is white in order to minimize short-wave radiation effects by warming (Hopkins 1996). Long-wave radiation may also affect the sensor in that bodies surrounding it, for example the ground, clouds, or the balloon, may warm or cool the sensor depending on the ambient air temperature. Generally, radiation effects are greater in the stratosphere, where differences can be up to 1 °C or more, than in the troposphere, where differences can be up to a few tenths of a degree (Dupilka 2006). The thermistor can measure temperatures that range from approximately -40 °C to 90 °C (Hopkins 1996).

Ambient water vapor, or humidity, is measure by a hygristor. The sensor measures relative humidity directly by means of a glass slide or plastic strip

covered with a moisture sensitive film of lithium chloride (LiCl) whose resistance changes with a change in atmospheric humidity (Hopkins 1996). The humidity sensor is located within the instrument package in such a way that outside air will pass over it while attempting to protect it from effects caused by liquid and frozen precipitation within and below precipitating clouds (Dupilka 2006).

Wind measurements are gathered using rawinsondes by receiving signals from fixed transmitting stations on the ground or from moving satellites in space. These signals are either retransmitted by the rawinsonde to the ground or are processed into Doppler-shift velocities and then transmitted (Dupilka 2006). In this way, balloon position and wind data are collected.

Measurements of pressure, temperature, humidity and wind gathered by balloon-borne rawinsondes are always subject to errors. The most common limitations of sensors include sensor time lag and hysteresis (Dupilka 2006). As the balloon ascends, instantaneous changes occur in the ambient environment and a sensor's time lag is the time it takes for a sensor to respond to such changes, which can be significant. Sensor lag affects mainly temperature and humidity sensors. For temperature sensors, the time lag is typically on the order of seconds, though humidity sensors may lag anywhere from seconds to minutes, especially when the balloon passes through steep humidity gradients at temperatures lower than -40 °C (Dupilka 2006). Hysteresis error occurs when the sensor fails to cycle from an initial value to another value, and then back again to the original value. This is especially prevalent for humidity sensors since the vertical profile of humidity is highly variable in the lower troposphere

(Dupilka 2006). Wright (1997) summarized the range, accuracy, precision and resolution of various rawinsonde measurements in Table A.

Table A: The range, accuracy, precision and resolution of various rawinsonde measurements. Adapted from Wright 1997.

Variable	Range	Accuracy	Precision	Resolution
Air Temperature	- 90 °C to + 50 °C	0.5 °C	0.40 °C for 1050-20 mb 1.00 °C <20 mb	0.1 °C
Relative Humidity	1 to 100 %	5 %	2.5 % for 100 – 30 % R.H. 3.5 % for 29.9 – 1 % R.H.	1 %
Wind Speed	0 to 225 kt	3 kt	6 kt	1 kt
Wind Direction	360 °	5 °	Varies with wind speed	1 °
Atmospheric Pressure	1070 to 2 mb	2.0 mb for P > 300 mb 1.5 mb for 300 < P < 50 mb 1.0 mb for P < 50 mb	1.5 mb	0.1 mb for P > 50 mb 0.01 mb for P < 50 mb
Geopotential Height	1070-500 mb 500-300 mb 300-100 mb 100-10 mb 10-3 mb	< 10 m < 15 m < 20 m < 30 m < 50 m	< 10 m < 15 m < 20 m < 30 m < 50 m	1 m

As summarized in Table A, sensor limitations cause error in air temperature values on the order of 1% while humidity and wind errors are on the order of 5%. The various sensors are periodically sampled by the data encoding electronics which encode and transmit sensor signals. Radiosonde sampling rates are chosen in order to provide the most representative profile of the atmosphere and are presently in the one to six second range (Dupilka 2006).

Appendix B

Data Obtained by Radiosondes

Table B contains an example of the data typically observed by a radiosonde. This data describes the vertical structure, or profile, of the atmosphere over Buffalo, New York at 0000 UTC on April 21, 1996.

Table B: Sounding data at Buffalo, New York for 0000 UTC, 04 April, 1996.

Height (m – AGL)	Pressure (mb)	Temperature (°C)	Dewpoint (°C)	Relative Humidity (%)	Wind Direction (degrees)	Wind Speed ($m\ s^{-1}$)
0	977	15.6	12.7	83	0	0
61	970	15.3	10	71		
149	960	15.4	10.4	72		
238	950	17.7	11.3	66	234	15.3
329	940	18.2	10.4	60		
421	930	18.1	9.4	57		
514	920	18	8.7	55		
607	910	17.7	8.4	54		
701	900	16.9	7.9	55	235	22.7
892	880	15.4	7.1	58		
1087	860	13.7	6.2	61		
1186	850	12.9	5.8	62	228	23.7
1285	840	12	5.6	65		
1486	820	10.1	5.3	73		
1692	800	8.1	5	81	225	23.7
1900	780	6.2	3.9	85		
2113	760	4.5	1.9	83		
2330	740	2.9	0.3	83		
2552	720	1	-0.7	88		
2778	700	-0.6	-3.1	83	225	27.8
3009	680	-2.2	-6.8	71		
3246	660	-3.2	-13.6	44		
3489	640	-5.1	-17	38		
3738	620	-6	-24.2	22		
3993	600	-8.3	-25.6	23	220	27.3
4254	580	-10.6	-27.3	24		
4523	560	-13.1	-29	25		
4800	540	-15.5	-30.7	26		
5083	520	-17.6	-33.8	22		
5376	500	-19.5	-37.6	18	222	24.7
5679	480	-20.9	-38.5			
5992	460	-22.7	-39.9			

6315	440	-24.9	-41.7		
6651	420	-27.3	-43.4		
7003	400	-29.7	-45.3	238	32.5
7368	380	-30.8	-46.7		
7751	360	-31.4	-47.2		
8155	340	-32.8	-48.4		
8578	320	-35.4	-49.7		
9027	300	-38.7	-51.2	225	68.5
9496	280	-42.8	-51.5		
9989	260	-47.3	-55.5		
10513	240	-51.9	-59.7		
11073	220	-56.2	-63.9		
11679	200	-56.6	-64.5	218	45.2
12341	180	-59.5	-67.3		
13079	160	-58	-66.1		
13919	140	-59.2	-67.3		
14886	120	-56.6	-65.2	223	19.9
16028	100	-61.2	-69.6		

In order to study these data, the observed temperature, dewpoint and relative humidity at selected pressure levels are plotted on thermodynamic diagrams. Such diagrams are tools used daily by meteorologists to display these values graphically. Mathematical relationships between physical properties are accounted for in the arrangement of these diagrams in order for lengthy calculations to be avoided (Hopkins 1996). The thermodynamic diagram consists of five families of isolines or isopleths such as isobars (lines of constant pressure), isotherms (lines of constant temperature), isentropics or adiabats (lines of equal potential temperature) for both dry and moist air, as well as equisaturated lines of constant mixing ratio. The value of these diagrams lies in their speed and convenience to analyze large amounts of information. They allow meteorologists to forecast vertical stability in the atmosphere by providing stability indices which can be calculated and displayed quickly and easily. They also aid in analyzing other atmospheric processes such as the determination of

cloud height and the types of air masses present (Dupilka 2006). There are a very large number of diagrams which have been developed for specific purposes. The most common diagrams used in weather forecasting are the tephigram and the Skew $T - \log p$ diagram which are mathematical transformations of one another (Iribarne and Godson 1981).

The name "tephigram" originated from the original name "T-φ-gram" to describe the temperature (T) and entropy (φ) axes that make up the plot. The coordinates of the tephigram are temperature (T) and a logarithmic scale of potential temperature ($\ln\theta$) which is proportional to the specific entropy. Isotherms and adiabats on a tephigram are straight lines, whereas isobars are logarithmic and are thus curved. However, their curvature over the range of meteorological usage is very small. The other common diagram, Skew $T - \log p$, has coordinates of T (temperature) and a logarithmic scale of pressure ($-\ln p$). Isobars and isotherms are straight lines and the angles between $-\ln p$ and T depend on the scales used for the coordinate axes, typically 45°. Wind barbs are commonly plotted on the side of both types of diagrams to indicate the winds at different heights in the atmosphere.

Appendix C

Tornadic Storm Events in Ontario

Table C: Tornadic storm events in the Ontario dataset between 1961 and 1996. Storm events prior to 1961 were not included because upper-air data did not exist before this date. If separate locations in close proximity reported a tornado, it was taken to be a single event and the location at which the greatest damage occurred was used for the F-scale rating. In the case where multiple tornadoes occurred on the same day, the representative sounding was used only once and the highest F-scale rating was chosen.

Month	Day	Year	Time	Location	F-scale	Dist. from BUF (km)
4	17	1967	1557	Exeter	3	240
4	17	1967	1712	Woolwich	3	164
5	2	1983	--	SE of Sarnia	4	288
5	31	1985	1557	Shelburne	4	178
5	31	1985	1515	SW of Barrie	4	171
5	31	1985	1515	Fergus	3	171
5	31	1985	1515	North of Fergus	4	180
6	16	1986	1430	E of Bracebridge	3	237
4	20	1996	1800	Williamsford	3	237
4	20	1996	1810	Arthur	3	178
6	29	1981	--	North of Barrie	2	208
6	18	1984	1636	Orilla	2	271
6	27	1987	1500	Elgin	2	272
7	25	1989	1445	Caledoneia	2	94
6	20	1993	1520	no detailed location only London-Midlesex-Oxford	2	approx. 240
5	15	1961	--	Wallacetown	1	225
6	1	1961	2100	Sherkson	1	34
6	23	1965	1700	North of Udney	1	196
5	17	1967	--	South of Dickson Hill	1	121
6	11	1968	1900	West of Brackenrig	1	254
6	11	1968	1800	Greenock	1	249
6	11	1968	1805	Dundalk	1	196
6	11	1968	1900	Stoneleigh	1	260
6	11	1968	1700	Mactier	1	233
6	13	1969	45	NW of Wellington	1	155
6	28	1976	1710	Forest	1	264
6	29	1976	1500	Hagersville	1	104
6	10	1979	1825	Brampton	1	120
6	26	1980	1510	Near Brent, Algonquin NP	1	119
6	26	1980	1740	Palmerston	1	200
3	30	1981	1300	Southwest Middlesex	1	267
6	22	1982	1750	Crediton	1	238
5	15	1988	2000	Nottawasaga Bay	1	176
7	7	1989	--	Napanee	1	205

7	12	1992	2100	Bayfield, Hu	1	252
8	1	1993	1500	near Port Perry	1	133
6	7	1995	1700	Uxbridge	1	140
5	20	1996	1950	Pelham	1	53
5	20	1996	1920	Stoney Creek	1	79
5	20	1996	1900	Paris	1	139
2	3	1961	1700	Alden, NY	0	17
6	10	1962	2100	Mapleton	0	184
5	27	1964	2110	West of York	0	127
5	6	1966	1400	Westport	0	269
6	16	1966	1500	Hamilton	0	97
4	21	1968	2100	Coppins Corners	0	132
5	25	1970	1730	Richmond Hill	0	121
5	25	1970	1630	East of Wingham	0	202
6	11	1970	1310	St. Catharines	0	55
6	6	1971	1300	East of Sarnia	0	292
6	15	1974	1330	NE of Sarnia	0	289
6	26	1976	1430	Victoria Road	0	178
6	28	1977	1500	Adjala	0	160
5	20	1978	1250	Fergus	0	167
6	1	1978	2100	Huron East	0	228
6	12	1978	1550	Youngstown	0	49
6	12	1978	1400	West of Gilmour	0	222
5	5	1980	1900	Stratford	0	193
5	5	1980	1940	East of Tavistock	0	170
5	5	1980	1900	Hensall	0	233
5	31	1980	--	North of Haliburton	0	245
5	31	1980	1234	Georgetown	0	127
6	10	1981	1257	South of Acton	0	132
7	18	1981	1655	North of Lincoln	0	92
5	19	1982	1323	Waldemar	0	166
5	19	1982	1333	Waldemar	0	166
6	20	1982	2330	NW of Port Dover	0	125
7	18	1982	1400	Starkville	0	121
7	28	1982	1445	West Hamilton	0	105
5	14	1987	1815	Mornington	0	192
7	24	1987	1730	Mississauga	0	107
5	2	1992	1745	Tavistock	0	177
5	17	1992	1745	Hickson	0	173
5	17	1992	1930	Hagersville	0	108
5	17	1992	1545	Pt. Clarke	0	275
8	14	1995	1710	Innisfil	0	171
4	26	1996	1800	Pickering	0	114
5	1	1996	1530	Primrose	0	174
7	8	1996	1830	Etobicoke	0	111
9	12	1996	1835	Beaverton	0	172

Appendix D

Hail Conversion

Table D: Hail conversion chart adapted from Moran, 2006 and the National Weather Service Southern Region Headquarters website at: http://www.srh.noaa.gov/tbw/html/tbw/skywarn/hail.htm

Hailstone Size	Diameter (cm)	Updraft Speed ($m\ s^{-1}$)
Pea	0.64	11
Marble	1.3	16
Dime	1.8	17
Penny	1.9	18
Nickel/mothball	2.2	21
Quarter	2.54	22
Half dollar	3.2	24
Walnut/Ping Pong Ball	3.8	27
Golf Ball	4.4	29
Hen Egg	5.1	31
Tennis Ball	6.4	34
Baseball	7.0	36
Tea Cup	7.6	38
Grapefruit	10.2	44
Softball	13.7	46

Appendix E

Eliminations of Tornado Events

Table E: Large outliers removed from the Ontario dataset and the corresponding date, F-scale rating and storm category.

Parameter	Value	Date	F-scale	Category
MUCAPE	7516 J kg^{-1}	May 16, 1988	F1	WT
BRN	896	June 12, 1968	F1	WT
BRN	445	July 25, 1987	F0	WT
SHR8	20.4403 m s^{-1} km^{-1}	April 27, 1996	F0	WT

Other comments regarding data eliminations:

MUCAPE less than 50 J kg^{-1} removed.
Storm convergence and BRN values equal to zero removed.
Storms at unknown times included.
Storms at unknown distances not included.